J|A|C|S
ARTICLES
Published on Web 05/23/2002

Long-Lived Charge-Separation by Retarding Reverse Flow of Charge-Balancing Cation and Zeolite-Encapsulated $Ru(bpy)_3^{2+}$ as Photosensitized Electron Pump from Zeolite Framework to Externally Placed Viologen

Yong Soo Park, Eun Jung Lee, Yu Sung Chun, Young Deok Yoon, and Kyung Byung Yoon*

Contribution from the Center for Microcrystal Assembly and Department of Chemistry, Sogang University, Seoul 121-742, Korea

Received March 20, 2002

Abstract: K^+-exchanged, $Ru(bpy)_3^{2+}$-encapsulating zeolite-Y [K^+-$Ru(bpy)_3^{2+}$Y] and *N*-[3-(dicyclohexylmethyl)oxypropyl-*N*′-methyl-4,4′-bipyridinium [DCH-MV^{2+}] were prepared, and visible light-induced electron transfer from the zeolite-encapsulated Ru(II) complex to the size-excluded viologen was studied in acetonitrile. Addition of a series of crown ethers (CEs) into the heterogeneous solution leads to over a 10-fold increase in the yield of DCH-$MV^{\bullet+}$, where the yield linearly increases as the formation constant of CE with K^+ [$K_f(K^+)_{CE}$] increases. The following two sequential events are attributed to be responsible for the above novel phenomenon. First, K^+ ions are liberated from the zeolite to solution during interfacial electron transfer from the photoexcited Ru(II) complexes to DCH-MV^{2+}. Second, the liberated K^+ ions form strong host−guest complexes with the added CE molecules, which leads to retardation of the reverse flow of the cations, hence the charge-balancing electrons, from the solution to the zeolite. Surprisingly, the yield of DCH-$MV^{\bullet+}$ reaches more than ∼50 times the amount of $Ru(bpy)_3^{2+}$ situated in the outermost supercages, despite the absence of electron relay in the zeolite. This is attributed to photosensitized electron pumping from the zeolite framework to viologen by the outermost $Ru(bpy)_3^{2+}$ ions. In support of the above conclusion, $Ru(bpy)_3^{3+}$ does not accumulate in the zeolite host while DCH-$MV^{\bullet+}$ accumulates in the supernatant solution. Consistent with the above, the independently prepared hexafluorophosphate salt of $Ru(bpy)_3^{3+}$ is reduced to $Ru(bpy)_3^{2+}$ in acetonitrile upon contact with $Ru(bpy)_3^{2+}$-free M^+Y (M^+ = Li^+, Na^+, K^+, Rb^+, and Cs^+), where the yield increases as the donor strength of the framework oxygen increases. Although small, thermal electron transfer also takes place from the zeolite framework to DCH-MV^{2+}, where the yield increases upon increasing the donor strength of the framework, concentration of DCH-MV^{2+}, temperature, and $K_f(K^+)_{CE}$ (when K^+Y is the zeolite host). The photoyield is always higher than the thermal yield by 4−30 times, confirming that the zeolite-encapsulated $Ru(bpy)_3^{2+}$ serves as the photosensitized electron pump.

Introduction

The spatial separation of the intimate ion pair (D^+,A^-) generated by photoinduced electron transfer (PET) from a donor (D) to an acceptor (A) is commonly referred as charge separation (CS). The ability to induce and maintain the charge-separated state (CSS) is essential for the vitality of the natural and artificial light energy harvesting systems.[1] One way to achieve long-lived CSS is to retard the energy wasting thermal back electron transfer (TBET) from the intimate ion pair, namely the electron transfer (ET) from A^- to D^+ (eq 1).[1−18]

$$D + A \underset{\text{TBET}}{\overset{\text{PET}}{\rightleftharpoons}} \underset{\text{intimate ion pair}}{[D^+, A^-]} \overset{\text{CS}}{\rightleftharpoons} \underset{\text{CSS}}{D^+ + A^-} \qquad (1)$$

As a possible means to demonstrate the strategies aimed to achieve long-lived CSS, zeolites have often been employed as

(1) Fox, M. A., Chanon, M., Eds. *Photoinduced Electron Transfer*; Elsevier: New York, 1988.
(2) Ramamurthy, V., Ed. *Photochemistry in Organized and Constrained Media*; VCH: New York, 1991.
(3) Kalyanasundaram, K. *Photochemistry in Microheterogeneous Systems*; Plenum: New York, 1987.
(4) Yoon, K. B. In *Solid State and Surface Photochemistry*; Ramamurthy, V., Schanze, K. S., Eds.; Marcel Dekker: New York, 2000; Vol. 5, Chapter 4.
(5) Yoon, K. B. *Chem. Rev.* **1993**, *93*, 321.
(6) Kim, Y. I.; Mallouk, T. E. *J. Phys. Chem.* **1992**, *96*, 2879.
(7) Krueger, J. S.; Mayer, J. E.; Mallouk, T. E. *J. Am. Chem. Soc.* **1988**, *110*, 8232.
(8) Yonemoto, E. H.; Kim, Y. I.; Schmehl, R. H.; Wallin, J. O.; Shoulders, B. A.; Richardson, B. R.; Haw, J. F.; Mallouk, T. E. *J. Am. Chem. Soc.* **1994**, *116*, 10557.
(9) Dutta, P. K.; Incavo, J. A. *J. Phys. Chem.* **1987**, *91*, 4443.
(10) Kalyanasundaram, K. *Coord. Chem. Rev.* **1982**, *46*, 159.
(11) Borja, M.; Dutta, P. K. *Nature* **1993**, *362*, 43.
(12) Bossmann, S. H.; Turro, C.; Schnabel, C.; Pokhrel, M. R.; Payawan, L. M., Jr.; Baumeister, B.; Wörner, M. *J. Phys. Chem. B.* **2001**, *105*, 5374.
(13) Sykora, M.; Kincaid, J. R. *Nature* **1997**, *387*, 162.
(14) Bhuiyan, A. A.; Kincaid, J. R. *Inorg. Chem.* **2001**, *40*, 4464.
(15) Fukuzumi, S.; Urano, T.; Suenobu, T. *Chem. Commun.* **1996**, 213.
(16) Persaud, L.; Bard, A. J.; Campion, A.; Fox, M. A.; Mallouk, T. E.; Webber, S. E.; White, J. M. *J. Am. Chem. Soc.* **1987**, *109*, 7309.
(17) Kim, Y. I.; Keller, S. W.; Krueger, J. S.; Yonemoto, E. H.; Saupe, G. B.; Mallouk, T. E. *J. Phys. Chem.* **1997**, *101*, 2491.
(18) Hurst, J. K.; Thompson, D. H. P.; Connolly, J. S. *J. Am. Chem. Soc.* **1987**, *109*, 507.

prototypical organizing media for a variety of D and A pairs for systematic PET reactions.[2−18] Prominent among these are the interfacial PET reactions from the photosensitized donors situated on the external surfaces of zeolites to the acceptors in zeolites[6−8] or from the photosensitized donors encapsulated in zeolites to the acceptors dissolved in solution.[11−15]

Mallouk and co-workers demonstrated that PET readily takes place from $Ru(bpy)_3^{2+}$ (bpy = 2,2′-bipyridine) placed on the external surfaces of zeolites (Y, L, and mordenite) to MV^{2+} ions incorporated within the pores.[6] The PET takes place much more readily when N,N′-ethylene-2,2′-bipyridinium ($2DQ^{2+}$) is tethered, as the electron relay, to one of the bpy ligands of the Ru(II) complex and when the relay is intercalated into the channels of L incorporating viologen acceptors.[7] The rate of PET decreases upon increasing the length of the spacer between the Ru(II) complex and the electron relay.[8] The above results demonstrate that the spatial organization of the photosensitized donor and the corresponding acceptor at the external and internal surfaces of zeolites, respectively, leads to much longer-lived CSSs [$Ru(bpy)_3^{3+}$,$V^{\bullet+}$] as compared to those in which the D and A pairs are placed in the neighboring cages of Y[9] or in homogeneous solutions.[10] It was also demonstrated that introduction of promethazine cation (PMZ^+), a size-excluded secondary electron donor, in solution (CH_3CN) ultimately leads to CS between the oxidized form of PMZ^+ (PMZ^{2+}) in solution and $MV^{\bullet+}$ in zeolite.[8] In this case, the Ru(II) complex on the external surface of the zeolite behaves as a photosensitized electron pump from PMZ^+ ($E° = 1.18$ V vs NHE in CH_3CN) to MV^{2+} ($E° = -0.21$ V vs NHE in CH_3CN), since the ET does not take place otherwise.

The PET from zeolite-encapsulated Ru(II) complexes to viologen acceptors placed in the supernatant solution has also received great attention. For instance, Dutta[11] and co-workers employed $Ru(bpy)_3^{2+}$ as the zeolite-encapsulated photosensitized donor [$E° = -0.87$ V in the triplet metal-to-ligand charge-transferred (^{3}MLCT) excited state, in H_2O vs NHE] and propyl viologen sulfonate (PVS, $E° = -0.41$ V in H_2O vs NHE) as an electron acceptor dissolved in water. The photoyield of the CSS between $Ru(bpy)_3^{3+}$ and $PVS^{\bullet-}$ increases dramatically when *N*,*N*′-tetramethylene-2,2′-bipyridinium, ($4DQ^{2+}$, $E° = -0.65$ V in H_2O, vs NHE) is incorporated as the electron relay into every empty supercage of Na^+Y. Thus, $4DQ^{2+}$ promotes electron conduction from every photoexcited $Ru(bpy)_3^{2+}$ [$*Ru(bpy)_3^{2+}$] in Na^+Y to PVS in solution.

Bossmann and co-workers demonstrated that TiO_2 nanowires incorporated within the interior of Y also serve as the electron relay between the zeolite-encapsulated $Ru(bpy)_3^{2+}$ and a size-excluded Co(III) complex placed in solution.[12]

It was demonstrated that the placement of an electron richer secondary donor adjacent to a photosensitized primary donor gives rise to further increase in the photoyield of CSS. For instance, Kincaid[13] and co-workers demonstrated that further increase (∼4-fold) in the photoyield of CSS results when a stronger donor [$Ru(4\text{-mmb})_3^{2+}$, 4-mmb = 4-methyl-2,2′-bipyridine, $E° = 1.18$ V vs NHE] is elegantly placed into the supercages adjacent to those occupied by a photosensitized donor [$Ru(bpy)_2bpz^{2+}$, bpz = bipyrazine, $E° = 1.50$ V in H_2O vs NHE]. The key idea of this work is to immediately reduce the oxidized form of the photosensitized donor, $Ru(bpy)_2bpz^{3+}$, back to the reduced state, $Ru(bpy)_2bpz^{2+}$, by the stronger donor [$Ru(4\text{-mmb})_3^{2+}$] in the adjacent supercage. Overall, $Ru(bpy)_2bpz^{2+}$ acts as a photosensitized electron pump from $Ru(4\text{-mmb})_3^{2+}$ to PVS. This eventually leads to slower TBET from $PVS^{\bullet-}$ to $Ru(4\text{-mmb})_3^{3+}$, which is a weaker acceptor than $Ru(bpy)_2bpz^{3+}$. Similarly, it has been demonstrated that the photoyield of $MV^{\bullet+}$ obtained from the Y incorporating MV^{2+} and two Ru(II) complexes with different $E°$ values, $Ru(bpy)_2bpz^{2+}$ and $Ru(bpy)_2(H_2O)^{2+}$ ($E° = 0.63$ V in H_2O vs NHE), in the adjacent cages is 4 times higher than that from the Y incorporating MV^{2+} and only one Ru(II) photosensitizer, $Ru(bpy)_3^{2+}$.[14]

Fukuzumi et al.[15] demonstrated long-lived CSS between Fe^{3+} in zeolite-Y and the anion radical of 7,7,8,8-tetracyanoquinodimethane ($TCNQ^{\bullet-}$) in solution, arising from ET from Fe^{2+} ions exchanged in zeolite-Y to TCNQ in acetonitrile by employing simultaneously exchanged *N*-methylacridinium (AC^+) as the photosensitized electron pump.

Mallouk and co-workers have also made efforts to exploit the advantages of the spatial separation of D−A systems on and in zeolites for H_2 generation from water.[16,17] For this purpose, Zn(II)−porphyrin complexes tethering intercalatable electron relays were employed as the externally placed photosensitized electron pumps for eventual ET from ethylenediaminetetraacetic acid (EDTA), a sacrificial electron donor in solution, to the internally incorporated MV^{2+} and Pt aggregates.[16] It was revealed that incorporation of TiO_2 or Nb_2O_5 semiconductor as the electron mediator between the photosensitized electron pump and MV^{2+} leads to a marked increase in the quantum yield.[17]

Hurst and co-workers[18] employed vesicles instead of zeolites as the organizing media as a means to provide insights into the long-lived CS. For instance, they demonstrated that the triplet excited state of the negatively charged zinc(II) porphyrin complex [5,10,15,20-tetrakis(4-sulfonatophenyl)porphinato]-zinc(II) (^{3}*$ZnTPPS^{4-}$) undergoes ET quenching by the long-alkyl chain viologen ions (C_nMV^{2+}), despite that they are incorporated into the negatively charged dihexadecyl phosphate (DHP) vesicles (C_nMV^{2+}-DHP). However, the lifetime of CSS ($ZnTPPS^{3-}$, C_nMV^+) increases significantly when the viologen radical cation is placed within the negatively charged vesicle, as a result of facile dissociation of the ion pair into free ions due to charge repulsion between the negatively charged $ZnTPPS^{3-}$ and C_nMV^+-incorporating DHP vesicles. The utilization of electrostatic repulsion between DHP vesicles and $ZnTPPS^{3-}$ for long-lived CS in the above system is likened to that between the negatively charged zeolite framework (Z^{n-}) and $PVS^{\bullet-}$ in the systems of Dutta, Kincaid, and their co-workers[11,13] and that between Z^{n-} and $TCNQ^{\bullet-}$ in the system of Fukuzumi and co-workers.[15]

None of the above reports, however, paid attention to the phenomenon of simultaneous movement of the charge-balancing cations (often alkali metal ions) during the interfacial PET and TBET, except the one by Dutta and co-workers, which discussed the possible role of the simultaneously migrating charge-balancing cation during intercage ET from $*Ru(bpy)_3^{2+}$ in a supercage of Y to MV^{2+} in the neighboring supercages.[19] Accordingly, no attempts have been made to explore the possible routes to achieve long-lived CSS by blocking the reverse flow of charge-balancing cations during TBET. We now report that a charge-balancing cation is indeed liberated from the interior

(19) Dutta, P. K.; Turbeville, W. *J. Phys. Chem.* **1992**, *96*, 9410.

Table 1. Composition of M^+Y Zeolites Used in This Study and the Yields of DCH-$MV^{\bullet+}$ and $Ru(bpy)_3^{2+}$ Produced from DCH-$MV^{2+}(PF_6^-)_2$ and $Ru(bpy)_3^{3+}(PF_6^-)_3$, Respectively, upon Contact with the Zeolite Powders[a]

M^+Y	composition	$-\delta_O$[b]	DCH-MV^{2+} [c]	$Ru(bpy)_3^{3+}$ [c]
Li^+Y	$Li_{37}Na_{16}Al_{53}Si_{139}O_{384}$	0.238	0	46
Na^+Y	$Na_{53}Al_{53}Si_{139}O_{384}$	0.265	1	175
K^+Y	$K_{49}Na_4Al_{53}Si_{139}O_{384}$	0.276	2	251
Rb^+Y	$Rb_{35}K_{13}Na_2H_3Al_{53}Si_{139}O_{384}$	0.284	4	501
Cs^+Y	$Cs_{37}K_{14}Na_2Al_{53}Si_{139}O_{384}$	0.304	6	2620

[a] 10 mg of each calcined zeolite powder was stirred for 24 h in 5 mL of 5.4 mM acetonitrile solution of DCH-$MV^{2+}(PF_6^-)_2$ or 1.3 mM acetonitrile solution of $Ru(bpy)_3^{3+}(PF_6^-)_3$ under anaerobic conditions. [b] Sanderson's partial negative charge density on the framework oxygen. [c] Yields are expressed as the number of ions per 100 unit cells of each zeolite.

of zeolite to the solution during interfacial ET from a zeolite-encapsulated photosensitized donor to an acceptor placed in solution, and over a 10-fold increase in the photoyield of CSS can be readily achieved through complexation of the liberated cation with a multiple chelating agent such as crown ether (CE). During the course of demonstrating the above strategy, we also discovered a novel phenomenon where dehydrated Z^{n-} acts as the electron donor to a viologen acceptor and $Ru(bpy)_3^{3+}$ in CH_3CN and, as a result, the zeolite-encapsulated $Ru(bpy)_3^{2+}$ acts as a photosensitized electron pump from Z^{n-} to the viologen in solution.

Results and Discussion

$Ru(bpy)_3^{2+}$ was chosen as the prototypical photosensitized electron donor encapsulated in zeolite-Y. Encapsulation of the Ru(II)-complex in K^+-exchanged zeolite-Y (K^+Y) was carried out according to well-established procedures.[20−24] The unit cell composition of K^+Y used for incorporation of $Ru(bpy)_3^{2+}$ is described in Table 1. The loading of $Ru(bpy)_3^{2+}$ was 54 μmol per gram of the dried zeolite, which corresponds to one $Ru(bpy)_3^{2+}$ per every 10 supercages.

As a means to embody a true interfacial ET from the zeolite-encapsulated $Ru(bpy)_3^{2+}$ complexes to an electron acceptor placed in solution, we prepared the hexafluorophosphate salt of *N*-[3-(dicyclohexylmethyl)oxypropyl]-*N*′-methyl-4,4-bipyridinium [DCH-$MV^{2+}(PF_6^-)_2$] as a bulky, size-excluded electron acceptor (see the Experimental Section for the synthetic procedure).

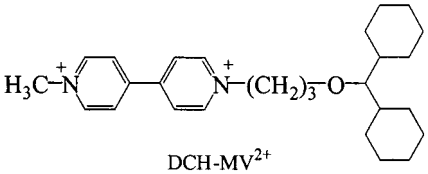

DCH-MV^{2+}

The kinetic diameter (minimum cross sectional width) of the acceptor ion was estimated to be 9.1 Å,[25] which is larger than the size of the aperture of zeolite-Y supercage (7.4 Å). Thus, due to the bulky dicyclohexylmethyl unit tethered to one of the sidearms of the viologen, the access of the viologen into the interior of the zeolite-Y is supposed to be denied. Indeed, analysis of the supernatant solution of the stirred (48 h) acetonitrile solution of DCH-$MV^{2+}(PF_6^-)_2$ (15 mL) suspended with K^+-exchanged zeolite-Y (K^+Y, 50 mg, 196 μmol of K^+) revealed that the exchanged amount varies only from 0.34 to 0.38% (from 0.66 to 0.74 μmol) of the total K^+ ions in K^+Y, despite the increase in the total amount of DCH-$MV^{2+}(PF_6^-)_2$ in the solution from 0.6 μmol (equivalent to 1.2 μmol of K^+) to 3.1 μmol (equivalent to 6.2 μmol of K^+). Thus, the ion exchange of K^+ in K^+Y with DCH-MV^{2+} is saturated at around 0.4%. This contrasts with the fact that all of the PF_6^- salt of methyl viologen, *N*,*N*′-dimethyl-4,4-bipyridinium [$MV^{2+}(PF_6^-)_2$], is exchanged into K^+Y under the identical conditions (50 mg of K^+Y, 0.6 and 3.1 μmol of $MV^{2+}(PF_6^-)_2$, respectively, in 15 mL of CH_3CN). Furthermore, in the case of $MV^{2+}(PF_6^-)_2$, the exchange level easily reaches to 20% upon stirring K^+Y (50 mg) with 20 mL of 11 mM solution of the salt. Therefore, it is concluded that the access of DCH-MV^{2+} into the supercage of K^+Y is denied by the supercage window and the exchange of the bulky ion is limited only onto the external surfaces of the zeolite particles.

Effect of CE on the Photoyield of DCH-$MV^{\bullet+}$. We first hypothesized that charge-balancing cations (K^+) should leave the zeolite host to solution during interfacial ET from $*Ru(bpy)_3^{2+}$ to DCH-MV^{2+} as a means to compensate for the loss of a negative charge in the zeolite host. As a corollary, TBET from DCH-$MV^{\bullet+}$ to $Ru(bpy)_3^{3+}$ should accompany the reverse migration of the liberated K^+ ions in solution back to the zeolite host. We further hypothesized that introduction of various CEs into the acetonitrile solution will form complexes with the liberated K^+ ions, which will eventually lead to retardation of TBET, since CEs are known to form strong complexes with alkali metal ions through chelation.[26] The CEs employed for this purpose are *cis*-dicyclohexano-18-crown-6 (DCH-18C6), 18-crown-6 (18C6), and 15-crown-5 (15C5), and their formation constants for complexation with K^+ [K_f(CE-K^+)] are $10^{6.6}$, $10^{5.7}$, and $10^{3.0}$, respectively.[27]

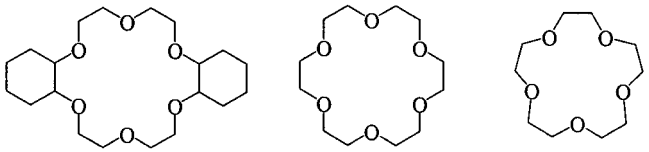

DCH-18C6 18C6 15C5

The estimated kinetic diameters of the CEs in the uncomplexed states are 10.3 Å (DCH-18C6 and 18C6) and 9.3 Å (15C5), respectively.[25] Therefore, they are all size excluded by the zeolite-Y aperture (7.4 Å). In fact, 18C6 and 15C5 have often been employed as templates for the synthesis of high-silica and hexagonal zeolite-Y.[28] When they are employed for this purpose, the CEs complexed with K^+ or Na^+ always remain trapped within the supercages of the resulting zeolites, due to their sizes being larger than those of the apertures. Accordingly, calcination of the resulting zeolites under flowing oxygen has

(20) (a) DeWilde, W.; Peeters, G.; Lunsford, J. H. *J. Phys. Chem.* **1980**, *84*, 2306. (b) Quayle, W. H.; Lunsford, J. H. *Inorg. Chem.* **1982**, *21*, 97.
(21) Incavo, J. A.; Dutta, P. K. *J. Phys. Chem.* **1990**, *94*, 3075.
(22) Dutta, P. K.; Turbeville, W. *J. Phys. Chem.* **1992**, *96*, 9410.
(23) Turbeville, W.; Robins, D. S.; Dutta, P. K. *J. Phys. Chem.* **1992**, *96*, 5024
(24) Laine, P.; Lanz, M.; Calzaferri, G. *Inorg. Chem.* **1996**, *35*, 3514.
(25) The kinetic diameter was estimated on the basis of the three-dimensional structure of the compound produced by the commercial program Chem-Draw.
(26) Gokel, G. W. *Crown Ethers and Cryptands*; The Royal Society of Chemistry: Cambridge, 1991.
(27) Izatt, R. M.; Bradshaw, J. S.; Nielsen, S. A.; Lamb, J. D.; Christensen, J. J. *Chem. Rev.* **1985**, *85*, 271.
(28) Delprato, F.; Delmotte, L.; Guth, J. L.; Huve, L. *Zeolites* **1990**, *10*, 546.

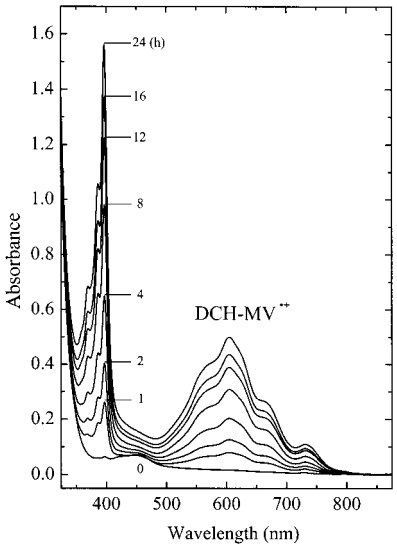

Figure 1. Progressive increase of DCH-$MV^{\bullet+}$ in the supernatant solution of DCH-$MV^{2+}(PF_6^-)_2$ upon irradiating a pellet of K^+-$Ru(bpy)_3^{2+}$Y at 450 ± 20 nm in the presence of DCH-18C6.

been a routine practice for removal of the encapsulated CEs from the resulting zeolites. This fact further verifies that the CEs cannot pass the supercage windows of zeolite-Y also in the complexed state.

To test the hypotheses, a thin, round, and self-supporting pellet (d = 7 mm) made from 10 mg of the dry, K^+-exchanged, $Ru(bpy)_3^{2+}$-incorporating zeolite-Y [K^+-$Ru(bpy)_3^{2+}$Y] [540 nmol of $Ru(bpy)_3^{2+}$] was placed in an airtight cell containing the acetonitrile solution of DCH-$MV^{2+}(PF_6^-)_2$ [MW = 698.5, 19 mg, 27 μmol, 50 equiv with respect to the amount of $Ru(bpy)_3^{2+}$] and DCH-18C6 (MW = 372.5, 6 mg, 16 μmol, 30 equiv). Upon irradiation of the pellet at the wavelengths of 430−470 nm using a 450-nm band-pass filter, the solution turned blue and the color intensified with time as irradiation continues. The UV−vis spectral measurement of the blue solution showed the characteristic spectrum of the viologen radical cation, DCH-$MV^{\bullet+}$, whose intensity progressively increased as shown in Figure 1.

The profile of the yield with respect to time is shown in Figure 2A. The yield of DCH-$MV^{\bullet+}$ with DCH-18C6 as CE after 24-h irradiation is 124 nmol, which corresponds to 23.0% with respect to the amount of $Ru(bpy)_3^{2+}$ present in the 10-mg pellet (540 nmol). The corresponding yield in the absence of the CE is 12 nmol (2.2%).[29] Thus, the addition of DCH-18C6 gives rise to as much as a 10.3-fold increase in the yield. The molar extinction coefficients (ϵ) of DCH-$MV^{\bullet+}$ independently measured in acetonitrile for the quantitative analysis of the radical cation are 46 500 and 12 690 M^{-1} cm^{-1} for 397- and 605-nm bands, respectively, which are quite comparable with those of $MV^{\bullet+}$ in acetonitrile.[30]

The irradiation angle also sensitively affects the overall yield for a given reaction period. Thus, even much higher yields (>50%) can be achieved within 24 h by carefully positioning the thin zeolite pellets vertically so that they can absorb incident light normal to the surface. However, due to the experimental difficulties to position the pellet normal to the incident beam of light repeatedly, the pellets were rather securely placed on a supporting glass plate placed within the cell, with a dihedral angle of 60° from the flat bottom of the rectangular cell.

Addition of less strongly complexing CEs such as 18C6 and 15C5 leads to a progressive decrease in the yield, as shown in Figure 2A. Thus, after 24 h of irradiation, the resulting yields are 15.8 and 7.4%, respectively. Figure 3A shows that there exists a linear relationship between the yield (taken after 24 h) of DCH-$MV^{\bullet+}$ and [K_f(CE-K^+)].

On the basis of the above results, we initially proposed Scheme 1 to account for the CE-dependent increase in the yield of CSS, employing DCH-18C6 as the prototypical CE. Thus, while the interfacial ET takes place from *$Ru(bpy)_3^{2+}$ to DCH-MV^{2+}, K^+ ions also leave the zeolite framework in order to maintain the overall charge balance in the zeolite system. The liberated K^+ ions then form strong host−guest complexes with DCH-18C6 [K_f(CE-K^+) = $10^{6.6}$]. Therefore, in order for the electron residing in DCH-$MV^{\bullet+}$ to return to the zeolite-encapsulated $Ru(bpy)_3^{3+}$, the K^+ ion should also return to the zeolite framework again to maintain the charge balance. However, since the CE complex of K^+ cannot pass through the zeolite-Y aperture (vide supra), the K^+ ions should first be decomplexed from the CE to return to the zeolite host to allow the interfacial TBET from DCH-$MV^{\bullet+}$ to $Ru(bpy)_3^{3+}$. Thus, as a result of the strong chelating power of the CE, the complexed K^+ ions can remain in solution for a longer period of time than in the absence of the CE, which causes retardation of the interfacial TBET from DCH-$MV^{\bullet+}$ to $Ru(bpy)_3^{3+}$. The linear relationship established between the yield and K_f(CE-K^+) in Figure 3 further verifies that the yield is governed by the complexing power of CE.

Alternatively, it can be imagined that DCH-MV^{2+} ions are first ion-exchanged onto the surface, and ET takes place mostly from *$Ru(bpy)_3^{2+}$ to the surface-exchanged DCH-MV^{2+} ions. Subsequently, the DCH-$MV^{\bullet+}$ ions generated on the surface are then exchanged with the unreduced ones (DCH-MV^{2+}) in solution. One might then propose that the presence of CEs with higher affinities for K^+ leads to an increase in the net concentration of the surface-exchanged DCH-MV^{2+} during ion exchange of K^+ ions on the zeolite surface with DCH-MV^{2+} in solution, which in turn leads to an increase in the yields of DCH-MV^{2+}. However, we found that the amounts of DCH-MV^{2+} ion exchanged onto the surface of K^+Y are nearly the same, regardless of the type of CE; thus, they are 0.44% (15C5), 0.46% (18C6), and 0.46% (DCH-18C6) of the total exchangeable cations in K^+. Therefore, the above alternative interpretation for the CE-dependent variation of yield of DCH-$MV^{\bullet+}$ can be excluded.

One of the requirements to establish Scheme 1 is to provide evidence that K^+ ions are indeed liberated from the zeolite host to solution with the amount equivalent to that of DCH-$MV^{\bullet+}$. To prove this, the reaction scale was increased by 10 times, and for this particular experiment, K^+-$Ru(bpy)_3^{2+}$Y was used in the powder form (see the Experimental Section for detail). The quantitative analysis of the supernatant solution at two different yields of DCH-$MV^{\bullet+}$, namely 564 and 993 nmol, revealed the presence of 568 and 1182 nmol of K^+ ion, respectively. Since the amount of K^+ ion liberated from K^+Y to solution through ion exchange of K^+ by DCH-MV^{2+} is negligible (vide supra), the above close matching between the

(29) The measurement of the quantum yield was not attempted since the reaction system is heterogeneous.
(30) Watanabe, T.; Honda, K. *J. Phys. Chem.* **1982**, *86*, 2617.

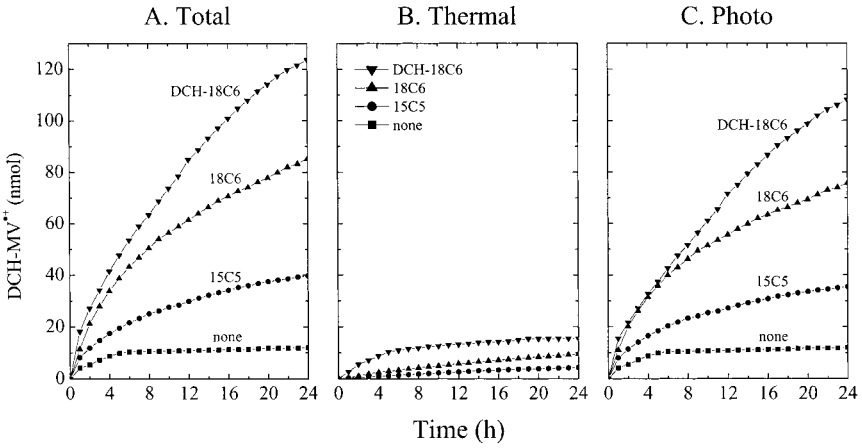

Figure 2. CE-dependent (as indicated) progressive increase in the total (A), the corresponding thermal (B), and the genuine photoinduced (C) yields of DCH-MV$^{\bullet+}$ with time.

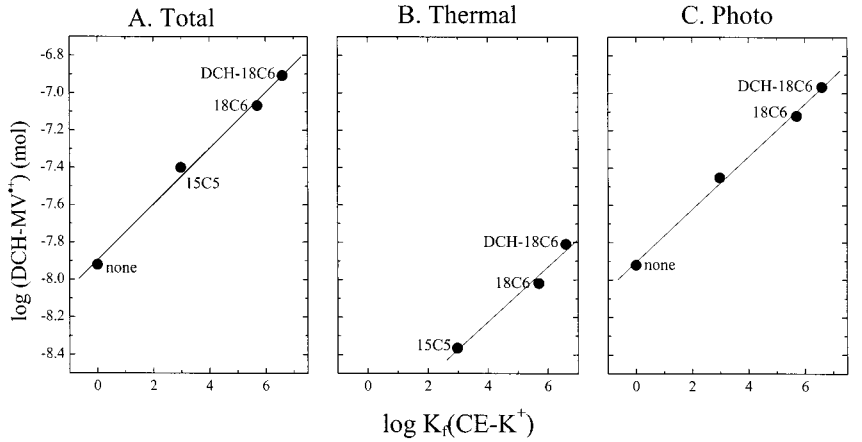

Figure 3. The linear relationship between the formation constant of CE with K^+ [K_f(CE-K^+)] and the total (A), the corresponding thermal (B), and photoinduced (C) yields of DCH-MV$^{\bullet+}$ after 24 h.

Scheme 1. Liberation of K^+ from the Zeolite Host to Solution at the Time of Interfacial ET from *Ru(bpy)$_3^{2+}$ to DCH-MV^{2+} and the Subsequent Complexation of the Liberated K^+ by DCH-18C6, as a Result of Photoexcitation (430−470 Nm) of K^+-Ru(bpy)$_3^{2+}$Y[a]

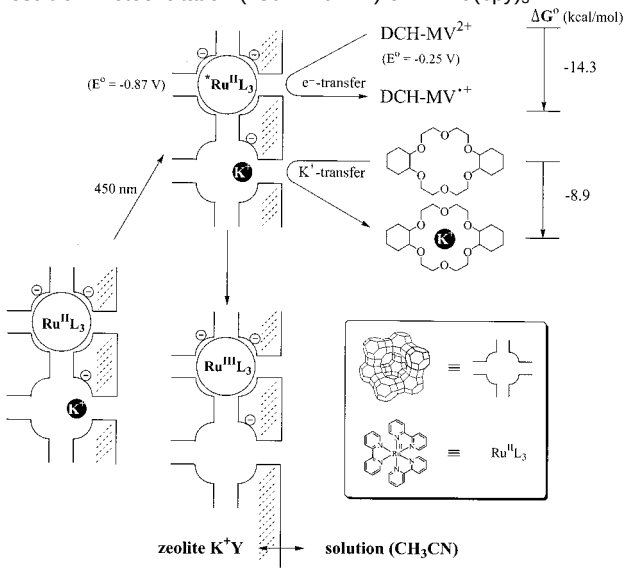

[a] E° Values Are Reported vs NHE in Acetonitrile

yield of DCH-MV$^{\bullet+}$ and the amount of K^+ in solution establishes that K^+ ions are indeed liberated from the zeolite framework to solution during the interfacial ET from *Ru(bpy)$_3^{2+}$ to DCH-MV^{2+} and they return to the zeolite framework during TBET from DCH-MV$^{\bullet+}$ to Ru(bpy)$_3^{3+}$.

Thermal ET from K^+-Ru(bpy)$_3^{2+}$Y and M^+Y to DCH-MV^{2+}. It is most likely that PET from *Ru(bpy)$_3^{2+}$ to DCH-MV^{2+} is limited to those Ru(II) complexes placed at the outermost supercages of zeolite-Y crystals. From the fact that the Ru complexes are homogeneously distributed within the interiors of zeolite crystals when the loading levels are less than or equal to two Ru complexes per three supercages,[24] it is reasonable to expect that about 1% of the total Ru(bpy)$_3^{2+}$ complexes in the K^+-Ru(bpy)$_3^{2+}$Y with the loading level of 1 Ru(bpy)$_3^{2+}$ per 10 supercages is situated at the outermost supercages of the zeolite particles. In this respect, considering that Z^{n-} is insulating, the observed yield (≥23.0%) of DCH-MV$^{\bullet+}$ in the presence of DCH-18C6 (after 24 h) is surprisingly high. This unexpected result suggests that there must be some sacrificial electron donors within the zeolite host, if not in solution, that keep regenerating Ru(bpy)$_3^{2+}$ from Ru(bpy)$_3^{3+}$. The control experiment with the zeolite-free solution containing only DCH-MV^{2+} and DCH-18C6 showed no indication of DCH-MV$^{\bullet+}$ formation, even after irradiation for 24 h, even by careful spectroscopic analyses. This verifies that there are no impurities in the solvent, DCH-MV^{2+}(PF_6^-)$_2$, and DCH-18C6 that serve as the electron donors to DCH-MV^{2+}. This therefore leads to the conclusion that sacrificial electron donors must reside *within* the zeolite host.

Interestingly, the control experiment in the dark revealed an interesting fact that about 13% (16 nmol) of the total yield originates from simultaneous thermal electron transfer (TET). This means that the genuine photoinduced yield of DCH-$MV^{\bullet+}$ after subtraction of the thermal yield (16 nmol) corresponds to 20% (108 nmol). This indicates that the yields shown in Figure 2A, actually represent the combined (total) yields originating from both TET and PET. The corresponding CE-dependent profiles of the thermal and the genuine photoinduced yields are shown in panels B and C of Figure 2, respectively. It was also revealed that the linear relationship also holds between K_f(CE-K^+) and the corresponding yield obtained either from TET or PET, as demonstrated in panels of B and C of Figure 3, respectively.

Zeolite Framework as Electron Donor. Knowing that $Ru(bpy)_3^{2+}$ does not thermally reduce DCH-MV^{2+} to DCH-$MV^{\bullet+}$ ($E°$ for $Ru(bpy)_3^{2+/3+}$ is 1.53 V[31] and that for DCH-$MV^{2+/\bullet+}$ is −0.25 V,[32] vs NHE in CH_3CN), the discovery of the TET process was highly intriguing. This, coupled with the aforementioned fact that the acetonitrile solutions of CEs contain no species that can reduce DCH-MV^{2+}, prompted us to examine K^+Y itself as a possible electron donor for DCH-MV^{2+}. For a more systematic study, we prepared a series of alkali metal-exchanged zeolites-Y (M^+Y, $M^+ = Li^+$, Na^+, K^+, Rb^+, and Cs^+) with the compositions listed in Table 1 (column 2), and they were calcined at 550 °C for 15 h under flowing oxygen to remove any organic contaminants. Immediately after calcination, they were evacuated at 350 °C for 10 h before they were finally transferred into a glovebox where an aliquot (10 mg) of each zeolite was introduced into a vial containing 5 mL of acetonitrile and DCH-$MV^{2+}(PF_6^-)_2$ (19 mg, 27 μmol).

Interestingly, although the presence of DCH-$MV^{\bullet+}$ was not visually apparent, the UV−vis analysis of the supernatant solutions from the acetonitrile suspensions of each zeolite powder stirred for 24 h in the dark revealed the presence of DCH-$MV^{\bullet+}$ in each solution. Furthermore, as listed in Table 1 (column 4), the produced amount of DCH-$MV^{\bullet+}$ progressively increased with increasing the size of M^+, where the amounts correspond to a few DCH-$MV^{\bullet+}$ radical ions, i.e., a few electrons per 100 unit cells of M^+Y.

Knowing that the formation of DCH-$MV^{\bullet+}$ cannot be attributed to the presence of electron-rich organic contaminants inadvertently present within the zeolites, as they were calcined (vide supra) prior to treatment with DCH-MV^{2+} under flowing oxygen, one might then alternatively suspect the transition metal impurities such as Fe(II) as the electron donors. Such a possibility is also very low, since the transition elements are likely to exist in their highest oxidation states after calcination. Furthermore, if there were still some transition elements capable of reducing DCH-MV^{2+}, the produced amount of DCH-$MV^{\bullet+}$ from each M^+Y should be nearly the same, since the zeolites are prepared from the same source (batch) of zeolite-Y.

Having concluded that there are no other candidates that could be assignable as electron donors, we now propose that Z^{n-} itself acts as the electron donor from the well-established fact that Z^{n-} can serve as the electron donor, and the donor strength of Z^{n-} increases with increasing the size or the electropositivity of the charge-balancing cation.[33−48] For instance, the results from the XPS studies[34−37] of Z^{n-}, the FT-IR studies of various probe molecules incorporated into zeolites,[38−42] the charge-transfer (CT) interactions between Z^{n-} and iodine[43] or MV^{2+} [44], and the UV−vis spectral shift of the arene donor−acceptor complexes encapsulated within zeolite hosts[45] have all served as solid experimental bases in establishing the fact that Z^{n-} serves as the electron donor and the donor strength of Z^{n-} increases with increasing the electropositivity of the charge-balancing cation.

There are numerous other examples that demonstrate the donor property of Z^{n-}. For instance, it has long been known that trinitrobenezene[49,50] and tetracyanoethylene[50,51] immediately form the corresponding anion radicals upon contact with Na^+Y, even at room temperature. It has been demonstrated that ET takes place from the framework to photosensitized electron acceptors such as pyrene,[52−54] tetracyanobenezene,[55] 1,4-dicyanobenzene,[55] pyromellitic dianhydride,[55] and methyl viologen (MV^{2+}).[56] In close relation to the above, zeolite frameworks have been known to eject electrons upon exposure to high-energy radiations such as γ-ray,[57] X-ray,[58] electron beams,[59,60]

(31) Ghosh, P. K.; Brunschwig, B. S.; Chou, M.; Creutz, C.; Sutin, N. *J. Am. Chem. Soc*. **1984**, *106*, 4772.

(32) The $E°$ values for $Ru(bpy)^{2+/3+}$ and DCH-$MV^{+/2+}$ were measured in acetonitrile using Ag/Ag^+ electrode as the reference. $LiClO_4$ (0.1 M) was used as the electrolyte. As for the filling solution of the reference electrode, $AgNO_3$ (0.01 M) was dissolved into the above $LiClO_4$ electrolytic solution. To each measured $E°$ value, 0.5082 V is added to convert the values with respect to NHE. See Mann, C. K.; Barnes, K. K. *Electrochemical Reactions in Nonaqueous Systems*; Marcel Dekker Inc.: New York, 1970; p 26.

(33) (a) Mortier, W. J.; Schoonheydt, R. A. *Prog. Solid St. Chem*. **1985**, *16*, 1. (b) Mortier, W. J. *J. Catal*. **1978**, *55*, 138. (c) Heidler, R.; Janssens, G. O. A.; Mortier, W. J.; Schoonheydt, R. A. *J. Phys. Chem*. **1996**, *100*, 19728. (d) Van Genechten, K. A.; Mortier, W. J. *Zeolites* **1988**, *8*, 273.
(34) (a) Barr, T. L.; Lishka, M. A. *J. Am. Chem. Soc*. **1986**, *108*, 3178. (b) Barr, T. L.; Chen, L. M.; Mohsenian, M.; Lishka, M. A. *J. Am. Chem. Soc*. **1988**, *110*, 7962. (c) Barr, T. L. *Zeolites* **1990**, *10*, 760.
(35) Okamoto, Y.; Ogawa, M.; Maezawa, A.; Imanaka, T. *J. Catal*. **1988**, *112*, 427.
(36) (a) Huang, M.; Adnot, A.; Kaliaguine, S. *J. Am. Chem. Soc*. **1992**, *114*, 10005. (b) Huang, M.; Adnot, A.; Kaliaguine, S. *J. Catal*. **1992**, *137*, 322.
(37) Kaushik, V. K.; Bhat, S. G. T.; Corbin, D. R. *Zeolites* **1993**, *13*, 671.
(38) (a) Barthomeuf, D. *J. Phys. Chem*. **1984**, *88*, 42. (b) Barthomeuf, D. *Stud. Surf. Sci. Catal*. **1991**, *65*, 157. (c) Murphy, D.; Massiani, P.; Franck, R.; Barthomeuf, D. *J. Phys. Chem*. **1996**, *100*, 6731.
(39) Huang, M.; Kaliaguine, S. *J. Chem. Soc., Faraday Trans*. **1992**, *88*, 751.
(40) (a) Barthomeuf, D.; Ha, B.-H. *J. Chem. Soc., Faraday Trans*. **1973**, *69*, 2158. (b) de Mallmann, A.; Barthomeuf, D. *Zeolites* **1988**, *8*, 292. (c) de Mallmann, A.; Barthomeuf, D. *J. Phys. Chem*. **1989**, *93*, 5636. (d) Dzwigaj, S.; de Mallmann, A.; Barthomeuf, D. *J. Chem. Soc., Faraday Trans*. **1990**, *86*, 431.
(41) Uytterhoeven, L.; Dompas, D.; Mortier, W. J. *J. Chem. Soc., Faraday Trans*. **1992**, *88*, 2753.
(42) (a) Mirodatos, C.; Pichat, P.; Barthomeuf, D. *J. Phys. Chem*. **1976**, *80*, 1335. (b) Mirodatos, C.; Abou Kais, A.; Vedrine, J. C.; Pichat, P.; Barthomeuf, D. *J. Phys. Chem*. **1976**, *80*, 2366.
(43) Choi, S. Y.; Park, Y. S.; Hong, S. B.; Yoon, K. B. *J. Am. Chem. Soc*. **1996**, *118*, 9377.
(44) Park, Y. S.; Um, S. Y.; Yoon, K. B. *J. Am. Chem. Soc*. **1999**, *121*, 3193.
(45) Hashimoto, S. *Tetrahedron* **2000**, *56*, 6957.
(46) Yashima, T.; Sato, K.; Hayasaka, T.; Hara, N. *J. Catal*. **1972**, *26*, 303.
(47) Ono, Y. *Stud. Surf. Sci. Catal*. **1980**, *5*, 19.
(48) (a) Hattori, H. *Chem. Rev*. **1995**, *95*, 537. (b) Tanabe, K.; Misono, M.; Ono, Y.; Hattori, H. *Stud. Surf. Sci. Catal*. **1989**, *51*, 1.
(49) Turkevich, J.; Ono, Y. *Adv. Catal*. **1969**, *20*, 135.
(50) Flockhart, B. D.; Mcloughlin, L.; Pink, R. C. *J. Catal*. **1972**, *25*, 305.
(51) Khulbe, K. C.; Mann, R. S.; Manoogian, A. *Zeolites* **1983**, *3*, 360.
(52) (a) Liu, X.; Iu, K.-K.; Thomas, J. K. *J. Phys. Chem*. **1994**, *98*, 7877. (b) Liu, X.; Iu, K.-K.; Thomas, J. K. *Chem. Phys. Lett*. **1993**, *204*, 163.
(53) Thomas, J. K. *Chem. Rev*. **1993**, *93*, 301.
(54) Iu, K.-K.; Thomas, J. K. *Colloids Surf*. **1992**, *63*, 39.
(55) Hashimoto, S. *J. Chem. Soc., Faraday Trans*. **1997**, *93*, 4401.
(56) McManus, H. J. D.; Finel, C.; Kevan. L. *Radiat. Phys. Chem*. **1995**, *45*, 761.
(57) (a) Liu, X.; Thomas, J. K. *Chem. Phys. Lett*. **1992**, *192*, 555. (b) Liu, X.; Thomas, J. K. *Langmuir* **1992**, *8*, 1750. (c) Liu, X.; Iu, K.-K.; Thomas, J. K. *J. Phys. Chem*. **1994**, *98*, 13720. (d) Iu, K.-K.; Liu, X.; Thomas, J. K. *J. Phys. Chem*. **1993**, *97*, 8165. (e) Liu, X.; Zhang, G.; Thomas, J. K. *J. Phys. Chem*. **1995**, *99*, 10024.
(58) Alvaro, M.; García, H.; García, S.; Marquez, F.; Scaiano, J. C. *J. Phys. Chem. B*. **1997**, *101*, 3043.
(59) (a) Liu, X.; Zhang, G.; Thomas, J. K. *J. Phys. Chem. B* **1997**, *101*, 2182. (b) Zhang, G.; Liu, X.; Thomas, J. K. *Radiat. Phys. Chem*. **1998**, *51*, 135. (c) Liu, X.; Mao, Y.; Ruetten, S. A.; Thomas, J. K. *Solar Energy Mater. Solar Cells* **1995**, *38*, 199.

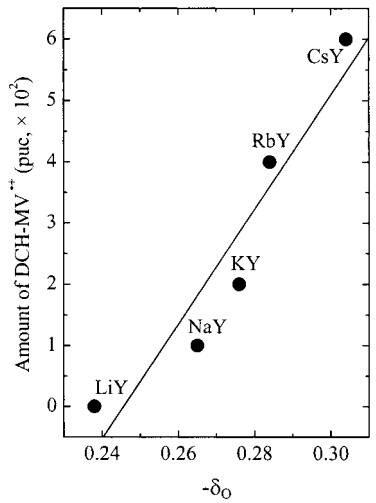

Figure 4. The linear relationship between the Sanderson's (average) partial negative charge on the framework oxygen ($-\delta_O$) of M^+Y (as indicated) and the yield of DCH-$MV^{\bullet+}$ produced from DCH-$MV^{2+}(PF_6^-)_2$ upon stirring with each zeolite powder in acetonitrile in the dark at ambient temperature in a glovebox charged with high-purity argon after 24 h.

and high-energy UV (such as 185, 193, and 248 nm).[56,61] The electrons generated from the framework by the high-energy radiations have been shown to reduce clusters of alkali metal ions (such as 4 Na^+),[57] MV^{2+},[56,57] and O_2.[59] Thus, the donor property of Z^{n-} has been unambiguously established.

In the meantime, the Sanderson's electronegativity equalization principle has served as a good theoretical basis to correlate between the experimentally observed donor strength of the framework and the calculated partial charge of the framework oxygen.[33] Although the yields are very small, we also found that there exists a good linear relationship between the Sanderson's partial negative charge density on the framework oxygen[62] of each M^+Y and the yield of DCH-$MV^{\bullet+}$, as shown in Figure 4. This relationship further supports our proposal that the zeolite framework indeed acts as the electron donor for DCH-MV^{2+}, and as a result, the degree of TET increases as the size of M^+ increases.

Although the yields in the absence of CEs are in fact very small, they become significant in the presence of CE_s, and the yield increases as K_f(CE-K^+) increases. For instance, as shown in Table 2 (column 2), the thermal yield of DCH-$MV^{\bullet+}$ increases in the presence of CE in the order none < 15C5 < 18C6 < DCH-18C6. The yield of DCH-$MV^{\bullet+}$ from K^+Y in the absence of any CE being smaller in Table 2 than that in Table 1 seems to arise due to the difference in the form of the zeolite; i.e., while the zeolites were used in the powder form in Table 1, they were used in pellets in Table 2. Table 2 also shows that

Table 2. CE-Dependent Change of Yield of DCH-$MV^{\bullet+}$ from K^+Y and K^+-Ru(bpy)$_3^{2+}$Y, Respectively[a]

	K^+Y	$[K^+$-Ru(bpy)$_3^{2+}]Y$		
CE	thermal[b]	thermal (T)[b]	photoinduced (P)[b]	P/T
none	0.0	0.0	1.6	
15C5	0.6	0.6	4.7	7.8
18C6	1.3	1.3	10.2	7.8
DCH-18C6	2.3	2.1	14.6	7.0

[a] A 10 mg pellet of each zeolite was placed in an airtight fluorescence cell containing 4 mL of acetonitrile solution of DCH-$MV^{2+}(PF_6^-)_2$ (50 equiv with respect to a unit cell of each zeolite) in the absence or in the presence of each CE (30 equiv), and the cell was placed in the dark (thermal) or under visible light (photoinduced) for 24 h at 30 °C. [b] Yields are expressed as the number of ions per 100 unit cells of each zeolite.

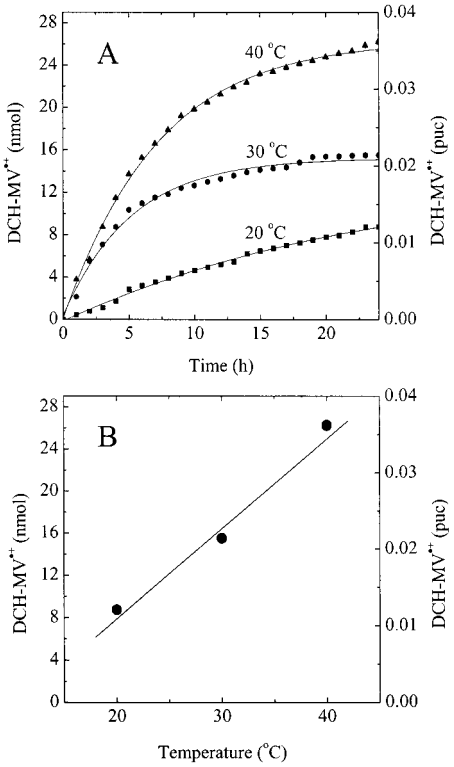

Figure 5. Plot of thermal yield of DCH-$MV^{\bullet+}$ from the mixture of DCH-$MV^{2+}(PF_6^-)_2$ and a pellet of K^+-Ru(bpy)$_3^{2+}$Y in acetonitrile with respect to time at different temperatures (A) and the linear relationship between the thermal yield taken after 24 h and different temperatures (B).

there is essentially no difference in the thermal yield, regardless of the presence (column 3) or absence (column 2) of Ru(bpy)$_3^{2+}$ in the zeolite. This further confirms that Ru(bpy)$_3^{2+}$ does not play any role during TET from Z^{n-} to DCH-MV^{2+}. This result also verifies that there are no remaining organic impurities in K^+-Ru(bpy)$_3^{2+}$Y capable of reducing DCH-MV^{2+}.

Effect of Temperature on Thermal Yield. We found that the ambient temperature sensitively affects the thermal yield. Thus, as displayed in Figure 5A, the thermal yield of DCH-$MV^{\bullet+}$ from K^+-Ru(bpy)$_3^{2+}$Y in the presence of DCH-18C6 increases with increasing the temperature of the reaction mixture over the entire reaction period of 24 h, and there is a linear relationship between the temperature and the yield of DCH-$MV^{\bullet+}$ taken after 24 h, as shown in Figure 5B. We also found that the yield obtained at 40 °C after 24 h slowly reduces to a value similar to the one obtained at 30 °C over a period of several days upon decreasing the temperature to 30 °C, which rises back to the initial value upon increasing the temperature

(60) Park, Y. S.; Um, S. Y.; Yoon. K. B. *Chem. Phys. Lett.* **1996**, *252*, 379.
(61) (a) Liu, X.; Iu, K.-K.; Thomas, J. K. *Chem. Phys. Lett.* **1994**, *224*, 31. (b) Liu, X.; Thomas, J. K. *J. Chem. Soc., Faraday Trans.* **1995**, *91*, 759.
(62) The Sanderson's (average) partial charge of the framework oxygen (δ_O) was calculated using the equation $\delta_O = (S_Z - S_O)/(2.08S_O^{1/2})$, where S_Z and S_O represent the Sanderson's intermediate electronegativity of each M^+-exchanged zeolite and the Sanderson's electronegativity of an oxygen atom. S_Z was calculated according to the equation $S_Z = (S_M{}^pS_{Si}{}^qS_{Al}{}^rS_O{}^t)^{1/(p+q+r+t)}$, where S_M, S_{Si}, and S_{Al} represent the Sanderson's electronegativities of the alkali metal cation, silicon, and aluminum, respectively, and *p*, *q*, *r*, and *t* represent the number of the corresponding element, respectively, in a unit cell. The following are the Sanderson's electronegativity for each element: Si, 2.14; Al, 1.71; O, 3.65; Li, 0.89; Na, 0.56; K, 0.45; Rb, 0.31; Cs, 0.22. The values were taken from: Huheey, J. E.; Keiter, E. A.; Keiter, R. L. *Inorganic Chemistry*, 4th ed.; Harper Collins College Publications: New York, 1993; pp 187ff.

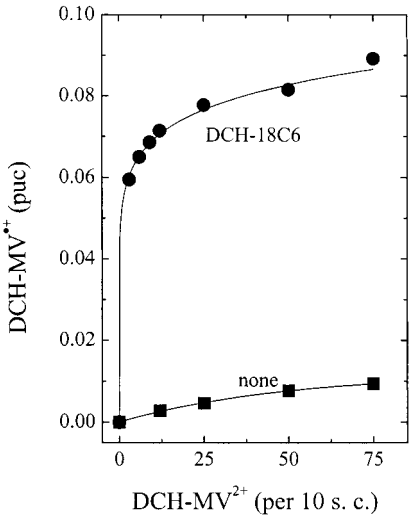

Figure 6. Plot of thermal yield of DCH-MV$^{\bullet+}$ from the mixture of DCH-MV^{2+}(PF_6^-)$_2$ and a pellet of K^+-Ru(bpy)$_3^{2+}$Y in acetonitrile with respect to the concentration of DCH-MV^{2+}(PF_6^-)$_2$ in the presence (top) and absence (bottom) of DCH-18C6 at 30 °C.

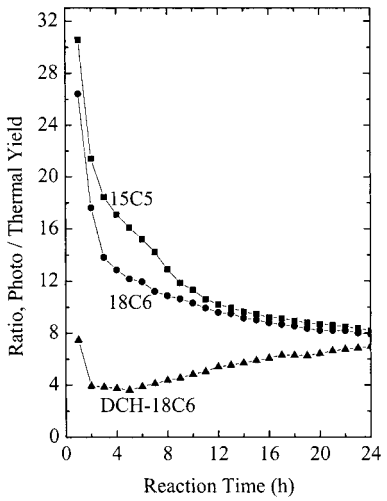

Figure 7. The time-dependent variation of the ratio of photo-to-thermal yields.

back to 40 °C. This indicates that the TET is an equilibrium reaction, as expressed in eq 2.

$$Z^{n-} + \text{DCH-MV}^{2+} \rightleftharpoons Z^{(n-1)-} + \text{DCH-MV}^{\bullet+} \qquad (2)$$

The above result also indicates that the equilibrium for TET from the framework to DCH-MV^{2+} shifts to the right upon increasing the temperature. In other words, the degree of temperature-induced increase in the rate of TET from Z^{n-} to DCH-MV^{2+} is higher than that from DCH-MV$^{\bullet+}$ to $Z^{(n-1)-}$. Knowing that the temperature sensitively affects the yield of DCH-MV$^{\bullet+}$, we therefore carried out all the reactions at 30 °C, unless specified otherwise.

The above result now sheds lights on the question we used to raise while working with MV^{2+}-exchanged Na^+Y (~1 MV^{2+} per supercage):[4,5,63] why does it develop a light blue color during evacuation at elevated temperatures, such as 150−200 °C, only to have the color slowly bleach with time upon cooling to room-temperature, despite the glass vessel containing the dried blue zeolite being stored in a glovebox charged with high-purity argon while the vacuum inside the glass vessel was maintained?

Effect of Concentration of DCH-MV^{2+} on Thermal Yield. We also found that the thermal yield of DCH-MV$^{\bullet+}$ from K^+Y increases with increasing the concentration of DCH-MV^{2+} in the supernatant solution, as shown in Figure 6. Although the presence of DCH-MV$^{\bullet+}$ in all of the supernatant solutions is always apparent from the spectroscopic analysis, it becomes visually detectable only when the yield reaches 0.08/unit cell (puc) or higher. Accordingly, visual observation of the pale blue coloration of the supernatant solution becomes possible only when the concentration of DCH-MV^{2+} is very high and in the presence of DCH-18C6. This indicates that one is apt to miss the presence (formation) of MV$^{\bullet+}$ in the acetonitrile solutions of MV^{2+} suspended with dry zeolites unless the concentration of MV^{2+} is extremely high or CEs are present in the solution.

Interestingly, the degree of concentration-dependent increase in the yield is also larger in the presence of DCH-18C6 than in its absence, i.e., while the yield of DCH-MV$^{\bullet+}$ increases to 0.09 in the presence of DCH-18C6, it increases only to 0.01 puc in the absence of the CE upon varying the concentration of DCH-MV^{2+} from 0 to 75 puc in the supernatant solution. This result, coupled with the larger increase in the overall yield, again emphasizes that the TET reaction is also effectively driven by complexation between K^+ and CEs.

As noticed, the yield of DCH-MV$^{\bullet+}$ does not linearly increase in both cases, and we confirmed the reproducibility of the nonlinear plot. Although the reason for the observed nonlinearity is yet to be elucidated, the above result further confirms that TET from Z^{n-} to DCH-MV^{2+} is an equilibrium reaction, as depicted in eq 2. This result also explains the unexplained phenomenon we used to observe while working with MV^{2+}-exchanged zeolites; the intensity of blue color developed on the zeolite at elevated temperatures is higher with increasing the degree of ion exchange of MV^{2+} in the zeolite. This result also explains why we did not observe MV$^{\bullet+}$ in our previous report regarding the charge-transfer interaction between MV^{2+} and the zeolite framework,[44] since the degree of MV^{2+} exchange in the zeolites for the previous work was only one out of eight supercages, which corresponds to 1 puc in the *X*-axis of Figure 6, where the amount of MV$^{\bullet+}$ is negligible, in particular, at room temperature.

Ru(bpy)$_3^{2+}$ as Photoinduced Electron Pump from Z^{n-} to DCH-MV^{2+}. Although it was demonstrated earlier that an equivalent amount of K^+ ion is liberated from the zeolite host to solution while DCH-MV$^{\bullet+}$ is generated in solution (vide supra), it is still necessary to prove that the stoichiometric amount of Ru(bpy)$_3^{3+}$ is simultaneously generated within the zeolite host during the PET from K^+-Ru(bpy)$_3^{2+}$Y to DCH-MV^{2+} to establish Scheme 1. However, despite our repeated trials, the characteristic ESR spectrum of Ru(bpy)$_3^{3+}$, which is supposed to give resonances at $g_\perp = 2.67$ and $g_{||} = 1.24$,[20b] was not detected, even from the K^+-Ru(bpy)$_3^{2+}$Y, which gave over 15% true photoyield of DCH-MV$^{\bullet+}$, while the supernatant solution showed a strong resonance at $g = 2.00$ due to DCH-MV$^{\bullet+}$ accumulated in the solution. Nevertheless, it is clear that the yield of DCH-MV$^{\bullet+}$ is always higher upon irradiation than not, as shown in Figure 7. Thus, the ratio of the photo-to-thermal yields of DCH-MV$^{\bullet+}$ initially ranges from 8 to 31 and then equilibrates to ~7 as the reaction time elapses (see column 5

(63) (a) Yoon, K. B.; Kochi, J. K. *J. Am. Chem. Soc.* **1989**, *111*, 1128. (b) Yoon, K. B.; Kochi, J. K. *J. Phys. Chem.* **1991**, *95*, 3780. (c) Yoon, K. B.; Huh, T. J.; Corbin, D. R.; Kochi, J. K. *J. Phys. Chem.* **1993**, *97*, 6492.

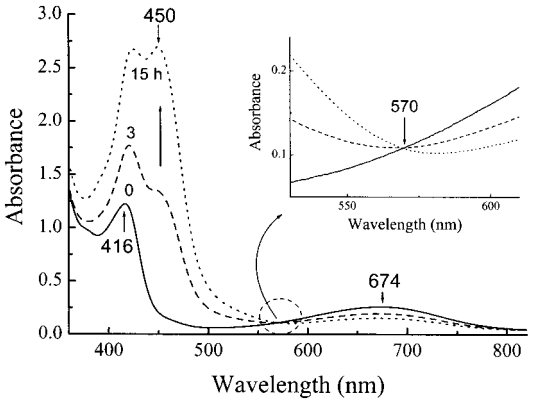

Figure 8. The spectrum (solid line) of $Ru(bpy)_3^{3+}(PF_6^-)_3$ in acetonitrile (0.6 mM, 5 mL) and the appearance and growth of the absorption of $Ru(bpy)_3^{2+}$ at 450 nm with time upon introduction of a pellet of K^+Y (10 mg) into the solution, after 3 (dashed line) and 15 h (dotted line), respectively. The inset shows an isosbestic point at 570 nm.

in Table 2). Therefore, the discrepancy that $Ru(bpy)_3^{3+}$ does not accumulate in the zeolite host while the yield of DCH-$MV^{\bullet+}$ keeps increasing in the supernatant solution, coupled with the one that the overall yield of DCH-$MV^{\bullet+}$ is much higher than the amount of $Ru(bpy)_3^{2+}$ present in the outermost supercages of Y, urged us to examine the reactivity of $Ru(bpy)_3^{3+}$ toward Z^{n-}.

For the above examination, we synthesized anhydrous $Ru(bpy)_3^{3+}(PF_6^-)_3$ by modification of the procedure reported by DeSimone and Drago.[64] It has been known that $Ru(bpy)_3^{3+}$ is stable only in strongly acidic solutions such as 6 M aqueous H_2SO_4 solution, but it is instantaneously reduced to $Ru(bpy)_3^{2+}$ by water in neutral aqueous media.[64] It has generally been believed that the powerful oxidant is also unstable in organic solvents such as acetonitrile.[64] However, we found that $Ru(bpy)_3^{3+}(PF_6^-)_3$ is in fact unlimitedly stable in acetonitrile at room temperature provided that the solvent is rigorously purified before use and the storage bottle is well capped in a moisture- and organic-vapor-free environment. For purification of the solvent, treatment with $KMnO_4$ is essential to remove the organic impurities that cause reduction of $Ru(bpy)_3^{3+}$ to $Ru(bpy)_3^{2+}$. Figure 8 shows the UV−vis spectrum of $Ru(bpy)_3^{3+}$ in acetonitrile. The absorption maximums appear at 416 ($\epsilon = 2\,230$) and 674 nm ($\epsilon = 410\ M^{-1}\ cm^{-1}$), closely matching with those of $Ru(bpy)_3^{3+}$ in acidic aqueous solutions, i.e., 418 ($\epsilon = \sim 3000$)[65] and 675 ($\epsilon = 440\ M^{-1}cm^{-1}$).[31] It is also worth noting that the molar extinction coefficient of the 416-nm band is about 6 times lower than that of the 450-nm band of $Ru(bpy)_3^{2+}$, which is 13 800 $M^{-1}cm^{-1}$ in acetonitrile.[66]

We found that the characteristic green color of $Ru(bpy)_3^{3+}$ slowly disappears from the solution, while the characteristic orange color of $Ru(bpy)_3^{2+}$ appears in the supernatant solution when a pellet of M^+Y is introduced into the acetonitrile solution of $Ru(bpy)_3^{3+}(PF_6^-)_3$. Again, the production of $Ru(bpy)_3^{2+}$ cannot be attributed to some organic contaminants inadvertently present in the zeolite hosts, since the M^+Y zeolites were calcined prior to introduction into the Ru(II) solution. Accordingly, we propose that Z^{n-} itself also acts as the electron donor to $Ru(bpy)_3^{3+}$ as it does even to a weaker electron acceptor, DCH-MV^{2+}. Monitoring of the supernatant solution containing a pellet of K^+Y by UV−vis spectrometry revealed that the rate of production of $Ru(bpy)_3^{2+}$ is slow but steady, as shown in Figure 8.

Scheme 2. A Diagram Showing the Role of $Ru(bpy)_3^{2+}$ as the Photoinduced Electron Pump for the Net ET Reaction from Z^{n-} to DCH-MV^{2+} and the Simultaneous Liberation of K^+ from the Zeolite Host to Solution and the Subsequent Complexation of the Cation by CE

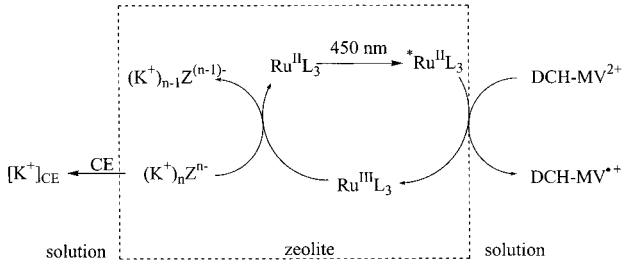

To achieve faster equilibrium, we added the acetonitrile solution of $Ru(bpy)_3^{3+}(PF_6^-)_3$ (5 mL, 2 mM) into each powder of M^+Y (10 mg), and the heterogeneous mixtures were stirred for 24 h. As listed in Table 1 (last column), analysis of the supernatant solution revealed that the yield of $Ru(bpy)_3^{2+}$, hence the number of electron liberated from the M^+Y, gradually increases from ∼0.5 to ∼5 puc of each zeolite as the size of M^+ increases from Li^+ to Rb^+, i.e., as the donor strength of Z^{n-} increases. When compared to the number of electrons liberated from each M^+Y to DCH-MV^{2+}, the numbers are at least 175 times larger. This can be rationalized from the fact that the acceptor strength of $Ru(bpy)_3^{3+}$ is much higher than that of DCH-MV^{2+}. Interestingly, Cs^+Y was exceptional and the amount of electrons liberated from the zeolite looks to be unusually high. A more detailed study is necessary to resolve the anomalous behavior of Cs^+Y.

ESR investigation of the $Ru(bpy)_3^{3+}$-treated M^+Y zeolites was also performed with the hope to detect the hole centers in the zeolites. However, all the zeolites, including the $Ru(bpy)_3^{3+}$-treated Cs^+Y, were ESR silent, even at 77 K. Consistent with our result, no reliable reports about the detection of hole centers in Z^{n-} have been made. The detection of the hole centers by ESR may not be possible if the electrons liberated from Z^{n-} for reducing DCH-MV^{2+} and $Ru(bpy)_3^{3+}$ come from the valence bands of insulating inorganic solids, from the view of band theory. Despite the loss of some electrons from Z^{n-}, analysis of the M^+Y zeolites with X-ray powder diffractometry showed that the structures (including Cs^+Y) remain intact.

On the basis of the above results we now propose that $Ru(bpy)_3^{2+}$ actually behaves as a photoinduced electron pump or photocatalyst for ET from Z^{n-} to DCH-MV^{2+} according to the scheme depicted in Scheme 2. First, $Ru(bpy)_3^{2+}$ reaches ^{3}MLCT excited state $^*Ru(bpy)_3^{2+}$ upon excitation. Among the $^*Ru(bpy)_3^{2+}$ complexes encapsulated within the zeolite hosts, those that reside in the outermost supercages of zeolite-Y then transfer electrons (one electron each) to DCH-MV^{2+} ions, perhaps through the contact at the zeolite apertures. The generated $Ru(bpy)_3^{3+}$ are then reduced back to $Ru(bpy)_3^{2+}$ by Z^{n-}. When an electron is discharged from $^*Ru(bpy)_3^{2+}$ to DCH-MV^{2+}, a charge-balancing cation K^+ is simultaneously liberated from the zeolite host to the external solution to maintain charge balance in the zeolite system. This is indispensable, since $Ru(bpy)_3^{3+}$ can balance three negative centers in the zeolite host.

(64) DeSimone, R. E.; Drago, R. S. *J. Am. Chem. Soc*. **1970**, *92*, 2343.
(65) Braddock, J. N.; Meyer, T. J. *J. Am. Chem. Soc*. **1973**, *95*, 3158.
(66) Young, R. C.; Meyer, T. J.; Whitten, D. G. *J. Am. Chem. Soc*. **1976**, *98*, 286.

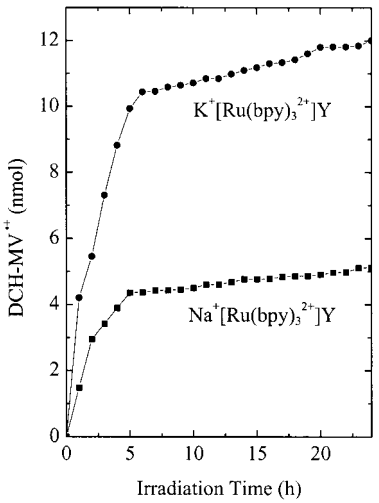

Figure 9. Increase in the photoinduced yield of DCH-$MV^{\bullet+}$ from the mixture of DCH-$MV^{2+}(PF_6^-)_2$ and a pellet of M^+-$Ru(bpy)_3^{2+}$Y at 30 °C upon changing the countercation (M^+) from Na^+ to K^+.

Upon reduction of $Ru(bpy)_3^{3+}$ to $Ru(bpy)_3^{2+}$, a positive charge is transferred from $Ru(bpy)_3^{3+}$ to the framework. Accordingly, Z^{n-} becomes $Z^{(n-1)-}$. Independent from ET from Z^{n-} to $Ru(bpy)_3^{3+}$, the liberated K^+ ion undergoes complexation with one of the CEs residing outside the zeolite hosts through chelation.

The above scheme coincides well with the absence of $Ru(bpy)_3^{3+}$ within the zeolite host, despite the continual increase of the true photoinduced yield of DCH-$MV^{\bullet+}$ in solution, with the facts that the yield of DCH-$MV^{\bullet+}$ is always higher upon irradiation than not and that the photoinduced yield is much higher than the amount of $Ru(bpy)_3^{2+}$ residing in the outermost supercages. On the basis of Scheme 2, DCH-$MV^{\bullet+}$ has to now undergo TBET to the oxidized form of Z^{n-} [$Z^{(n-1)-}$] but not to $Ru(bpy)_3^{3+}$. Since $Z^{(n-1)-}$ is a much weaker electron acceptor than $Ru(bpy)_3^{3+}$, as judged by the facile ET from Z^{n-} to $Ru(bpy)_3^{3+}$, the corresponding thermodynamic driving force for the ET from DCH-$MV^{\bullet+}$ to $Z^{(n-1)-}$ is much less than that from DCH-$MV^{\bullet+}$ to $Ru(bpy)^{3+}$. This situation is likened to the schemes of Mallouk and co-workers,[8] where the surface-exchanged Ru(II) complex acts as the photosensitized electron pump from the ultimate electron donor, PMZ^+, to MV^{2+}, and of Sykora and Kincaid,[13] where $Ru(bpy)_2bpz^{2+}$ acts as the photosensitized electron pump and $Ru(mmb)_3^{2+}$ as the neighboring ultimate electron donor to the oxidized form of the electron pump. Alternatively, in the respect that $Ru(bpy)_3^{2+}$ acts as the photoinduced electron relay, the situation is also closely related to the system of Fukuzumi and co-workers, in which AC^+ acts as the photoinduced electron relay from Fe^{2+} ions in zeolite-Y to TCNQ in solution.[15]

The fact that Z^{n-} is the ultimate electron donor is further supported by the experimental result that the photoinduced yield from K^+-$Ru(bpy)_3^{2+}$Y in the absence of any CE is also higher than that from Na^+-$Ru(bpy)_3^{2+}$Y, as shown in Figure 9, despite that the amount of $Ru(bpy)_3^{2+}$ loading in each zeolite is the same (1 per 10 supercages). If the framework serves only as an inert compartmentalizing host, then there would be no such difference in the yield, since the number of $Ru(bpy)_3^{2+}$ located in the outermost supercages is the same in both cases.

The reason for both PET and TET reactions being slow in our system may be attributed to slow propagation of the hole center in the framework initially generated at the periphery of the zeolite crystals into the interior. The temperature-induced increase in the rate demonstrated in Figure 5 may then arise due to faster propagation of the hole center in the framework.

Knowing that Z^{n-} can readily reduce $Ru(bpy)_3^{3+}$ from this work, now is the time to discuss the possibility whether Z^{n-} can also reduce the oxidized forms of the photosensitizers employed by Mallouk,[6−8,16,17] Dutta,[11] Kincaid,[13] and their co-workers. However, such a pathway is less likely in their systems, since the reactions were carried out in aqueous solutions and hydrated zeolite frameworks usually do not act as electron donors.[44] Instead, since their PET reactions are carried out in aqueous solutions, the possible role of water molecules as the sacrificial electron donors should be raised from the fact that $Ru(bpy)_3^{3+}$ is instantaneously reduced by water in nonacidic aqueous media, as mentioned earlier.[67]

Indeed, Lunsford,[20b] Dutta[68] and their co-workers prepared $Ru(bpy)_3^{3+}$-encapsulating Na^+Y and demonstrated that the Ru(III) complex is slowly reduced to $Ru(bpy)_3^{2+}$ upon contact with water. Therefore, in the systems of Mallouk,[6−8,16,17] Dutta,[11] Kincaid,[13] and their co-workers, water is likely to play the role of the secondary donors such as anhydrous Z^{n-} does in this paper, unless the reactions are carried out in highly acidic media, or in the presence of good secondary electron donors such as PMZ^+,[8] $Ru(4\text{-}mmb)_3^{2+}$,[13] $Ru(bpy)_2(H_2O)^{2+}$,[14] or EDTA.[16,17]

In the Fukuzumi and co-workers' system,[15] however, the simultaneous ET from Z^{n-} to $*AC^+$ should also be considered as a competitive route as well as the proposed ET from Fe^{2+} to $*AC^+$, since the reaction was carried out in acetonitrile. As a result, the CSS between $Z^{(n-1)-}$ and $TCNQ^{\bullet-}$ is likely to coexist together with the one between Fe^{3+} and $TCNQ^{\bullet-}$. Alternatively, the final CSS between Fe^{3+} and $TCNQ^{\bullet-}$ may also proceed via the one between $Z^{(n-1)-}$ and $TCNQ^{\bullet-}$.

The result shown in Figure 9 also indicates that the residual moisture present in the $Ru(bpy)_3^{2+}$Y, due to not high enough dehydration temperature (200 °C), does not play the role of secondary electron donor in our case, since the amount of residual moisture is likely to be higher with Na^+ as the countercation than K^+, in compliance with the well-known phenomenon that the electrostatic field strength in the vicinity of the cation is higher with decreasing the size.[69] Otherwise, the yield of DCH-$MV^{\bullet+}$ should be higher with Na^+ as the countercation than K^+.

The fact that $Ru(bpy)_3^{3+}$ can in fact be incorporated safely within Na^+Y (vide supra) as described above seems to contradict with our proposal that Z^{n-} reduces $Ru(bpy)_3^{3+}$. However, a careful analysis of the procedure to generate $Ru(bpy)_3^{3+}$ in Na^+Y resolves the discrepancy. Thus, generation of $Ru(bpy)_3^{3+}$ in Na^+Y has been carried out by treating the dried Na^+-

(67) The fact that water is readily oxidized by $Ru(bpy)_3^{3+}$ at neutral pHs is conceivable from the fact that the $E°$ value of water (1.23 V for 2 $H_2O \rightleftarrows O_2 + 4H^+ + 4e^-$ vs NHE; Bard, A. J.; Faulkner, L. R. *Electrochemical Methods: Fundmentals and Applications*; John Wiley & Sons: New York, 1980; p 700.) is lower than that of $Ru(bpy)_3^{3+}$, which can be obtained only in highly acidic aqueous solutions (1.26 V in 6 M aqueous H_2SO_4 solution vs NHE).

(68) (a) Ledney, M.; Dutta, P. K. *J. Am. Chem. Soc*. **1995**, *117*, 7687. (b) Das, S. K.; Dutta, P. K. *Langmuir* **1998**, *14*, 5121.

(69) (a) Rabo, J. A.; Angell, C. L.; Kasai, P. H.; Schomaker, V. *Discuss. Faraday Soc*. **1966**, *41*, 328−349. (b) Breck, D. W. *Zeolite Molecular Sieves*; Wiley: New York, 1974. (c) Dempsey, E. *J. Phys. Chem*. **1969**, *73*, 3660. (d) Dempsey, E. *Molecular Sieves*; Society of Chemical Industry, London, 1968; p 293. (e) Ward, J. W. In *Zeolite Chemistry and Catalysis*; Rabo, J. A., Ed.; ACS Monograph 171; American Chemical Society: Washington, DC, 1976; Chapter 3.

Scheme 3. A Simplified Version of Scheme 2 Showing Only the Net ET Reaction from Z^{n-} to DCH-MV^{2+} and the Liberation of K^+ from the Zeolite Host to Solution and the Subsequent Complexation of the Cation by CE

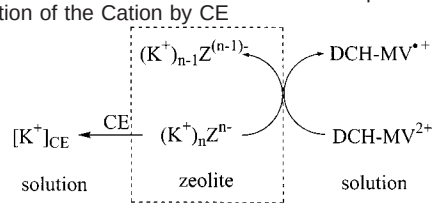

$Ru(bpy)_3^{2+}Y$ with chlorine gas, which has been known to oxidize Z^{n-} as well. For instance, it has been known that treatment of dry zeolites X and mordenite with chlorine results in the formation of Cl_2^-.[70] Now, considering the fact that the $E°$ of Cl_2 (1.36 V, in water vs NHE)[71] is higher than that of $Ru(bpy)_3^{2+}$,[67] it is expected that chlorine will oxidize the zeolite framework more readily than $Ru(bpy)_3^{3+}$ does. Therefore, it is highly reasonable to expect that all the valence electrons or the basic sites that could possibly be oxidized by $Ru(bpy)_3^{3+}$ are already removed by chlorine during formation of the Ru(III) complex, enabling the zeolite framework to host $Ru(bpy)_3^{3+}$.

From the conclusion that ET also takes place directly from Z^{n-} to DCH-MV^{2+} (vide supra), the pathway described in Scheme 3 also exists. Therefore, coupled with the result shown in Figure 7 and Table 2, it is now clear that there exist two pathways in yielding DCH-$MV^{\bullet+}$, photoinduced (Scheme 2) and thermal (Scheme 3). In the case of the former, $Ru(bpy)_3^{2+}$ acts as the electron pump. It is also worth noting that Scheme 3 also represents the net ET reaction described in Scheme 2.

For the electrons to be transferred from $*Ru(bpy)_3^{2+}$ to the external DCH-MV^{2+}, many possible mechanisms can be imagined. One way is to transfer an electron at the aperture of zeolite-Y through direct contact between the electron donor in the outermost supercage and the acceptor in solution. An alternative pathway is to inject an electron from $*Ru(bpy)_3^{2+}$ to the conduction band of Z^{n-} in the absence of water, and subsequently, the electron in the conduction band of Z^{n-} is then transferred to DCH-MV^{2+} at the terminal of the framework. If this is the case, then the role of the zeolite framework is likened to that of 4-DQ^{2+}, MV^{2+} tethered to the Ru(II) complexes, and the semiconductors such TiO_2 or Nb_2O_5 employed by Dutta,[11] Mallouk,[7,8] Bossmann,[12] and co-workers. However, for the ET from $*Ru(bpy)_3^{2+}$ to the conduction band of Z^{n-} to take place readily, the energy level of the conduction band of Z^{n-} should be lower than that of $*Ru(bpy)_3^{2+}$. Therefore, without knowing the precise energy level of the conduction band of Z^{n-}, further discussion is yet premature.

Thermodynamic Consideration of the CE-Dependent Yield. The effect of CE on the increase in the yield of DCH-$MV^{\bullet+}$ can also be analyzed from the thermodynamic point of view. With DCH-18C6 as the prototypical complexing agent, the estimated standard free energy change ($-\Delta G°$) for complexation of K^+ is 8.9 kcal mol^{-1}, which corresponds to 62% of the free energy change (14.3 kcal mol^{-1}) for ET from $*Ru(bpy)_3^{2+}$ to DCH-MV^{2+} if the forward ET occurs directly from $*Ru(bpy)_3^{2+}$ to DCH-MV^{2+}, as shown in Scheme 1. This means that the overall thermodynamic driving force for the reaction increases by 62% via simultaneous complexation of K^+ with the CE. Therefore, for such a reversible reaction like this case, complexation of K^+ by the CE renders the overall equilibrium of the ET reaction shift to the forward ET.

In summary, the present work reports the following novel experimental results. The zeolite framework (Z^{n-}) of alkali-metal-exchanged zeolite-Y (M^+Y) acts as an electron donor to DCH-MV^{2+} and $Ru(bpy)_3^{3+}$. The zeolite-encapsulated $Ru(bpy)_3^{2+}$ acts as a photosensitized electron pump from Z^{n-} to DCH-MV^{2+} in solution. The interfacial ET from the zeolite-encapsulated $*Ru(bpy)_3^{2+}$ or Z^{n-} to DCH-MV^{2+} in solution and the TBET from DCH-$MV^{\bullet+}$ to the oxidized form of Z^{n-} [$Z^{(n-1)-}$] accompany the simultaneous migration of the charge-balancing cation, M^+. Complexation of the M^+ liberated from the zeolite host to solution by CEs leads to long-lived CSS. A PET reaction can be driven forward by complexation of the simultaneously migrating cation with complexing agents.

Experimental Section

Materials. Na^+Y (LZY-52, Si/Al ratio = 2.6, Lot No. 968087061020-S) was purchased from Union Carbide. Hexaammineruthenium(III) chloride was purchased from Strem. Dicyclohexylmethanol, sodium hydride, allyl bromide, borane−tetrahydrofuran complex (1 M), triphenyl phosphite, methyl iodide, DCH-18C6, 18C6, 15C5, and 4,4′-bipyridine were purchased from Aldrich. 18C6 was recrystallized from hot water. Methyl iodide was distilled before use. Tetrahydrofuran (THF) was distilled over sodium-benzophenone prior to use. Acetontirile was stirred for 24 h in the presence of $KMnO_4$ until the purple color of the oxidant persists in the solution. The $KMnO_4$-treated acetonitrile was first simple distilled and then redistilled over P_2O_5 under argon. The distilled acetonitrile was transferred to a Schlenk flask using a Teflon cannular under argon atmosphere. The Schlenk flask was then stored in a glovebox charged with high-purity argon. Diethyl ether was stirred over the aqueous solution of $KMnO_4$ (diethyl ether:water = 9:1) for 15 h. The collected diethyl ether was washed with water and then treated with (concentrated) sulfuric acid for 15 h. The collected and water-washed diethyl ether was dried over anhydrous $CaCl_2$ and distilled over the eutectic mixture of sodium and potassium under argon. The distilled diethyl ether was also transferred into a Schlenk storage bottle under argon and kept in the glovebox. Na^+Y was washed once with 1 M NaCl solution to ensure incorporation of Na^+ as the charge-balancing cation. Li^+Y and K^+Y were prepared from Na^+Y by treating it with 1 M LiCl and KCl solutions, respectively, five times. Rb^+Y and Cs^+Y were prepared from K^+Y by treating it with 0.5 M RbCl and CsCl solutions, respectively, three times. The resulting zeolites after ion exchanges were washed with distilled deionized water until the silver ion test for chloride was negative. The washed, ion-exchanged zeolites were calcined at 550 °C for 10 h under flowing oxygen to remove organic impurities prior to use.

Incorporation of $Ru(bpy)_3^{2+}$ into the K^+-exchanged zeolite-Y was carried out according to the well-established procedure.[20−24] To remove $Ru(bpy)_3^{2+}$ complexes that might have formed on the external surface of the zeolite-Y crystals, the $Ru(bpy)_3^{2+}$-incorporating zeolites (10 g) were washed with aqueous KCl solution (0.1 M, 100 mL) for three times and subsequently with distilled deionized water until the silver ion test for chloride is negative. The analysis of the amount of $Ru(bpy)_3^{2+}$ in K^+-$Ru(bpy)_3^{2+}Y$ was initiated by dissolving the zeolite framework with 10% aqueous HF solution according to the reported procedure.[24] The analysis revealed that the loading of $Ru(bpy)_3^{2+}$ in K^+-$Ru(bpy)_3^{2+}Y$ is 1 Ru complex per 10 supercages. K^+-$Ru(bpy)_3^{2+}Y$ (10 mg each) was pressed into round, thin pellets (d = 7 mm) using a press at the pressure of 600 kgf cm^{-2}. The pellets of K^+-$Ru(bpy)_3^{2+}Y$ were dehydrated at 200 °C for 10 h under vacuum and then stored in a glovebox charged with high purity argon.

Preparation of DCH-MV^{2+}. As a means to prepare the viologen with a bulky sidearm that can prevent the access of the viologen in

(70) Coope, J. A. R.; Gardner, C. L.; McDowell, C. A.; Pelman, A. I. *Mol. Phys.* **1971**, *21*, 1043.
(71) See the reference in ref 67.

Scheme 4. A Synthetic Procedure to Prepare 3-(Dicyclohexylmethyl)oxy-1-iodopropane (1c)

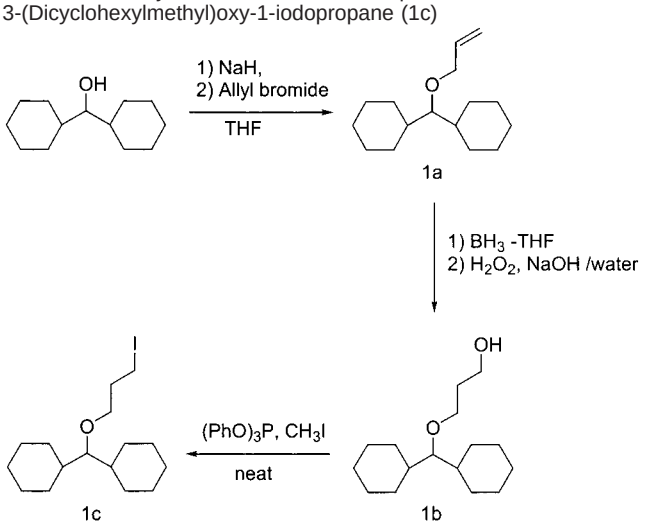

solution into the interior of the zeolite, 3-(dicyclohexylmethyl)oxy-1-iodopropane (Scheme 4, **1c**) was prepared with the intent to prepare DCH-MV^{2+}.

Preparation of Dicyclohexylmethyloxyallyl Ether (Scheme 4, 1a). The THF solution (90 mL) of dicyclohexylmethanol (7.46 g, 38.02 mmol) was added to a suspension of dry NaH (1.09 g, 45.60 mmol) in THF (30 mL) with vigorous stirring at room temperature. After 1-h reflux, the THF solution (30 mL) of allyl bromide (4.84 g, 40.01 mmol) was introduced into the above mixture, and the reflux was allowed to proceed for an additional 15 h with vigorous stirring. After cooling to room temperature, the precipitated NaBr was filtered off from the mixture and THF in the clear solution was removed by evaporation in vacuo. Into the flask containing the residue was introduced diethyl ether (200 mL) to dissolve the residue. The diethyl ether solution was washed successively with brine (30 mL) and water (30 mL) to remove the residual NaBr dissolved in the THF solution. The NaBr-free solution was dried using anhydrous $MgSO_4$ and concentrated in vacuo. The crude product was isolated by column chromatography (ethyl acetate:*n*-hexane = 1:36): $C_{16}H_{28}O$ 236.39; yield (6.37 g, 71%); ^{1}H NMR ($CDCl_3$, ppm) 5.98 (m, 1H), 5.25 (d, 1H), 5.08 (d, 1H), 4.03 (d, 2H), 2.78 (t, 1H), 1.22−1.85 (m, 22H).

Preparation of 3-(Dicyclohexylmethyl)oxypropan-1-ol (1b). A solution of BH_3−THF (22 mL, 1 M, 22 mmol) was added dropwise to a THF solution (10 mL) of **1a** (6.37 g, 26.97 mmol). The clear, colorless reaction mixture was stirred at room temperature for 30 min to complete the reaction. Excess hydride was destroyed by the careful addition of 5 mL of water. After the cease of hydrogen evolution, 10 mL of aqueous sodium hydroxide (3 M) was added to the reaction mixture and hydrogen peroxide (10 mL, 30% aqueous solution) was added dropwise to the stirred reaction mixture at a rate such that the temperature did not exceed approximately 40 °C. The reaction mixture was subsequently heated at 50 °C for 1 h to ensure complete oxidation. The reaction mixture was cooled to room temperature and most of the solvent (THF and water) was stripped off in vacuo. Distilled water (30 mL) was introduced into the flask containing the residue and **1b** was extracted from the aqueous slurry using diethyl ether three times (50 mL each). The diethyl ether solution was dried with anhydrous $MgSO_4$, and evaporation of the ethereal solution yielded **1b**. The crude product was purified by column chromatography (ethyl acetate:*n*-hexane = 1:9): $C_{16}H_{30}O_2$ 254.41; yield (5.60 g, 82%); ^{1}H NMR ($CDCl_3$, ppm) 3.82 (t, 2H), 3.71 (t, 2H), 2.68 (t, 1H), 1.14−1.95 (m, 25H).

Preparation of 1c. Triphenyl phosphite (7.09 g, 22.85 mmol), methyl iodide (4.05 g, 28.53 mmol), and **1b** (4.83 g, 18.99 mmol) were charged into a two-necked round-bottomed flask fitted with a Hg thermometer and a reflux condenser connected to a drying tube charged with calcium chloride. The neat reaction mixture was heated under gentle reflux until the temperature reached to about 130 °C, as a result of the consumption of most of the low boiling methyl iodide in the reaction mixture. It requires about 48 h to reach the temperature at which the reaction mixture turns dark and fuming becomes vigorous. The tarry reaction mixture was then cooled to room temperature and distilled water (50 mL) was added to the flask to remove polar byproducts. The residue was extracted with diethyl ether three times (50 mL each). The diethyl ether solution was dried using anhydrous $MgSO_4$ and the solvent was removed by evaporation. The crude product (**1c**) was isolated by column chromatography (ethyl acetate:*n*-hexane = 1:36): $C_{16}H_{29}IO$ 364.31; yield (6.13 g, 89%); ^{1}H NMR ($CDCl_3$, ppm) 3.51 (t, 2H), 3.31 (t, 2H), 2.66 (t, 1H), 2.06 (quintet, 2H), 1.80−1.14 (m, 22H).

Preparation of 1-Methyl-4-(4′-pyridyl) Pyridinium Iodide (MPP^+I^-). Methyl iodide (1.7 mL, 28 mmol, 1.25 equiv) was added to a dichloromethane solution of 4,4′-bipyridine (3.5 g, 22 mmol) and the reaction mixture was refluxed overnight. The produced yellow precipitate was isolated by filtration and subsequently purified by recrystallization from methanol and diethyl ether: $C_{11}H_{11}IN_2$ 298.13; yield (6.23 g, 95%); ^{1}H NMR (DMSO, ppm) 9.27 (d, 2H), 8.98 (dd, 2H), 8.74 (d, 2H), 8.17 (t, 2H), 4.52 (s, 3H).

Preparation of DCH-MV^{2+}(PF_6^-)$_2$. Into an acetonitrile solution (50 mL) of MPP^+I^- (1.1 g, 3.7 mmol) was added **1c** (1.48 g, 4.05 mmol, 1.1 equiv) and the solution was refluxed for 48 h. After cooling to room temperature, the red precipitate [DCH-MV^{2+}(I^-)$_2$] was isolated by filtration and dissolved in distilled deionized water. The aqueous solution (50 mL) of NH_4PF_6 (5 g) was added dropwise to the clean, pale yellow solution of the iodide salt of DCH-MV^{2+}. The precipitated, white hexafluorophosphate salt of DCH-MV^{2+} was isolated by filtration and recrystallized twice from acetonitrile and diethyl ether: $C_{27}H_{40}F_{12}N_2OP_2$ 698.56; yield (1.68 g, 65%); ^{1}H NMR (CD_3CN, ppm,) 8.99 (d, 2H), 8.89 (d, 2H), 8.40 (m, 4H), 4.79 (t, 2H), 4.45 (s, 3H), 3.68 (t, 2H), 2.71 (t, 1H), 2.33 (m, 2H), 1.80−1.14 (m, 22H)

Preparation of Ru(bpy)$_3^{3+}$(PF_6^-)$_3$. Ru(bpy)$_3^{3+}$(PF_6^-)$_3$ was synthesized using the procedure reported by DeSimone and Drago[64] by employing PbO_2 as the oxidizing agent in 6 M H_2SO_4 aqueous solution. The precipitated Ru(bpy)$_3^{3+}$(PF_6^-)$_3$ in the acidic solution was filtered over a glass frit and the filtered green powder (microcrystals) was immediately transferred into a glovebox charged with high purity argon. The surface of the green powder turned reddish during the course of transfer to the dry chamber. The reddish green powder (5 g) was dissolved into the rigorously purified acetonitrile (30 mL). The color of the solution was initially green but slowly turned orange with time. Upon addition of rigorously purified diethyl ether (150 mL), the solution slowly turned orange while green powder precipitates at the bottom of the flask. After standing still for 4 h in the glovebox, the supernatant solution was removed by decanting. The above procedure was repeated four additional times until the supernatant solution consists of diethyl ether and the acetonitrile was free of the orange hue due to the presence of Ru(bpy)$_3^{2+}$(PF_6^-)$_2$. The collected dark green powder (0.5 g) was kept in a glass vial. The UV−vis spectrum of the green powder dissolved in fresh acetonitrile did not show the characteristic 450-nm band of Ru(bpy)$_3^{2+}$ but only the 416- and 674-nm bands of Ru(bpy)$_3^{3+}$. The corresponding extinction coefficients were 2230 and 410 M^{-1} cm^{-1}, respectively.

PET from Zeolite-Encapsulated Ru(bpy)$_3^{2+}$ to DCH-MV^{2+} in Solution. In a glovebox charged with high purity argon, a piece of thin zeolite pellet (10 mg, d = 7 mm) was placed on a piece of glass plate (∼6 × 18 mm^2), which was placed in an airtight fused silica fluorescence cell. The dihedral angle between the supporting glass plate and the flat bottom of the rectangular cell was about 60°. An aliquot of an acetonitrile solution of each crown ether [2 mL, 8.1 mM, 30 equiv with respect to Ru(bpy)$_3^{2+}$] was introduced into the cell, and an additional 2 mL of acetonitrile solution of DCH-MV^{2+}(PF_6^-)$_2$ (13.5 mM, 50 equiv) was subsequently added. The airtight fluorescence cell was then brought out of the glovebox and exposed to visible light generated from a 200-W Hg lamp at the wavelengths between 430 and

470 nm using a 450-nm band-pass filter (Corion, P70−450-F), in a homemade temperature-controlled irradiation chamber. The temperature inside the chamber was controlled to 30 ± 1 °C. The solution was gently stirred during irradiation with the help of a small magnetic stirring bar placed under the tilted glass plate. The stirring did not cause disintegration of the pellet into powder. The solution turned blue upon irradiation, due to formation of DCH-$MV^{\bullet+}$, and the blue color intensified with time. After each 1-h period of irradiation, the cell was removed from the light source and the spectrum of DCH-$MV^{\bullet+}$ was measured on a UV−vis spectrophotometer. The fluorescence cell was placed in the cell holder in such way that the plane of the glass support in the cell lies parallel to the direction of the incident beam, to minimize the interference caused by the glass plate during the measurement of the yield. The sample pellets did not interfere the passage of the analyzing beam.

TET from Zeolite Framework to DCH-MV^{2+} in Solution. For this experiment all of the $Ru(bpy)_3^{2+}$-free M^+Y zeolites with different cations (either in the form of pellet or powder) were calcined separately from one another at 550 °C for 10 h under flowing oxygen. Immediately after calcination they were each transferred to a glass tube equipped with a greaseless stopcock and further evacuated in each tube at 350 °C for 10 h before they were finally transferred into a glovebox, where a pellet or an aliquot of each zeolite was introduced into a vial containing an acetonitrile solution of DCH-$MV^{2+}(PF_6^-)_2$.

A General Procedure. An airtight, fused silica fluorescence cell containing a piece of thin zeolite pellet (10 mg, $d = 7$ mm) of K^+-$Ru(bpy)_3^{2+}Y$, 2 mL of 8.1 mM acetonitrile solution of each CE [30 equiv with respect to the amount of $Ru(bpy)_3^{2+}$], and 2 mL of 13.5 mM acetonitrile solution of DCH-$MV^{2+}(PF_6^-)_2$ (50 equiv) was prepared similarly in the glovebox charged with high-purity argon. When CE is not required, 2 mL of pure acetonitrile was introduced into the cell instead of the CE solution. The cell was then placed in a water bath placed in a dark chamber. Both the water bath and the supernatant solution inside the cell were magnetically stirred with the aid of appropriate magnetic bars. The desired temperature (20, 30, and 40 °C) of the bath was controlled using an immersion heater/cooler. The spectral change of the supernatant solution was measured at ambient temperature in the dark by removing the cell from the bath, and the cell was placed back to the controlled temperature bath immediately after spectral measurement. The spectral measurement was performed every hour until the overall elapsed time reached 24 h. The surface of the cell was briefly cleaned using a tissue wetted with ethanol prior to each spectral measurement.

To obtain the effect of DCH-MV^{2+} concentration on the thermal yield, a weighed amount of DCH-$MV^{2+}(PF_6^-)_2$ was introduced into the cell containing a pellet of K^+Y and 4 mL of 4.05 mM acetonitrile solution of DCH-18C6. The amounts were 1.2 mg (3 equiv), 2.4 mg (6 equiv), 3.6 mg (9 equiv), 4.7 mg (12 equiv), 9.4 mg (25 equiv), 18.8 mg (50 equiv), and 28.3 mg (75 equiv with respect to 10 supercages of K^+Y).

To obtain the effect of countercation on the thermal yield, 10 mg of M^+Y (see Table 1) was introduced into a vial containing 5 mL of 5.4 mM solution of DCH-$MV^{2+}(PF_6^-)_2$ in the glovebox under a dimmed red light. The tightly capped vial was wrapped with aluminum foil to prevent light from going into the vial. The acetonitrile suspension of the vial was magnetically stirred for 20 h, and the zeolite powders were allowed to sediment during the period of 4 h. Subsequently, 4 mL of the clear supernatant solution was transferred to a fused silica UV−vis cell equipped with an airtight cap. The cell was removed from the glovebox for the spectral measurement.

Reaction of $Ru(bpy)_3^{3+}(PF_6^-)_3$ with Zeolite. Into a vial containing 5 mL of 1.3 mM acetonitrile solution of $Ru(bpy)_3^{3+}(PF_6^-)_3$ was introduced 10 mg of dried M^+Y (see Table 1) in the form of powder in the glovebox. The tightly capped vial was wrapped with aluminum foil to prevent light from going into the vial. The rest of the procedure is the same with that employed to investigate the effect of countercation on the thermal yield. In the case Cs^+Y, which consumed all of the $Ru(bpy)_3^{3+}$ complex present in the solution, an additional 5-mL aliquot of the Ru(III) solution was added into the vial containing the zeolite. For the in situ measurement of the spectral change from Ru(III) to Ru(II) in the presence of zeolite, a pellet of 10 mg of K^+Y was placed inside the fluorescence cell containing 4 mL of 0.65 mM acetonitrile solution of $Ru(bpy)_3^{3+}(PF_6^-)_3$, and the cell was placed in the light-protected compartment of a UV−vis spectrophotometer. The spectral change of the supernatant solution was monitored by taking the spectrum at a regular interval (1 h).

Quantitative Analysis of K^+ Liberated from Zeolite to Solution. For quantitative analysis of K^+, the scale of the reaction was increased by 10 and K^+-$Ru(bpy)_3^{2+}Y$ was used in powder form. The blue supernatant solution from the irradiated mixture was collected by filtration in the glovebox. The solution was then taken out of the glovebox and the solvent was removed by evaporation. Into the residual solid was added 20 mL of 1 M aqueous NH_4Cl solution to convert the hexafluorophosphate (PF_6^-) salt of K^+ and DCH-MV^{2+} into the corresponding water-soluble chloride (Cl^-) salts for the subsequent ICP-AES analysis of potassium.

Instrumentation. The X-ray diffraction patterns for the identification of the zeolite crystals were obtained from a Rigaku diffractometer (D/MAX-1C) with the monochromatic beam of Cu Kα. The UV−vis spectra of the samples were recorded on a Shimadzu UV-3101PC. The diffuse reflectance UV−vis spectra of solid samples were obtained using an integrating sphere. The solution ^1H and ^{13}C NMR spectra were recorded on a Varian Jemini 300 NMR spectrometer. Irradiation of the samples was carried out using a 200-W super high-pressure Hg lamp placed in an Oriel 66011 housing. The quantitative analysis of K^+ was carried out on a Shimadzu ICPS-1000 IV.

Acknowledgment. We thank the Ministry of Science and Technology (MOST), Korea, for supporting this work through the Creative Research Initiatives (CRI) program. We are also very grateful to the referees for the valuable comments and corrections that greatly helped improve the quality of this paper.

JA020446A